

MAX-PLANCK-INSTITUT FÜR PLASMAPHYSIK
GARCHING BEI MÜNCHEN

Model Calculations of the
Tearing Instability Associated with
AC-Modulation of the Plasma-Current in Tokamaks

F. Pohl
S. von Goeler*
W. Engelhardt
K. Lackner
M. Murmann

IPP 6/198

June 1980

IPP III/60

*On leave from Plasma Physics Laboratory of
University of Princeton
1st September, 1978 to 31st August, 1979

*Die nachstehende Arbeit wurde im Rahmen des Vertrages zwischen dem
Max-Planck-Institut für Plasmaphysik und der Europäischen Atomgemeinschaft über die
Zusammenarbeit auf dem Gebiete der Plasmaphysik durchgeführt.*

IPP 6/198
IPP III/60

F. Pohl
S. von Goeler
W. Engelhardt
K. Lackner
M. Murmann

Model Calculations of the Tearing
Instability Associated with AC-Modulation
of the Plasma-Current in Tokamaks

June 1980 (in English)

Abstract

The tearing mode stability of the radial profiles of current density resulting from the skin effect accompanying AC modulation is calculated using a computer code.

1. Introduction

On the Pulsator tokamak at Garching an experiment was performed in which an AC component was superposed on the plasma current [14,15]. To interpret and plan these experiments, a computer program to calculate the current distributions accompanying the AC modulation taking into account the skin effect was developed. The experiments showed that AC modulation of high amplitude impairs the plasma stability and can lead to disruption. Since tearing modes are believed to be responsible for the disruptive instability, calculations on the stability of these modes were performed.

This report presents a detailed description of the computer program and its results. Section 2 deals with the skin effect; Section 3 is a discussion of the stability of tearing modes. The heating effects associated with AC modulation are discussed in Section 4. Sections 5-8 document the computer program.

2. Radial Current Profile

Figure 1a shows a schematic drawing of the essential features of the experimental configuration. The ohmic heating transformer incorporates some supplementary windings in addition to the standard windings. These windings are powered by an AC-generator which is switched on at time t_1 during a tokamak discharge. As shown in Fig. 1b, the plasma current, I_p , and the loop voltage, V_{PL} , consist approximately of a stationary component originating from the standard power supply and, for $t \geq t_1$, of an AC component. In the calculations it is assumed that the AC component of the plasma loop voltage is periodic. The plasma current is calculated from the plasma loop voltage, V_{PL} . Immediately after the AC is switched on, the plasma goes through a transient state which lasts for a few cycles; afterwards, the AC component of the plasma current is also periodic.

The penetration of the alternating current into the plasma column is calculated under the following simplifying assumptions:

1. The toroidal plasma is treated like a cylinder.
2. The displacement current is neglected because of the low frequency of the AC component.
3. Because of the strong toroidal magnetic field, motions of the plasma are neglected so that Ohm's law has the simplified form

$$j_z = \sigma E_z \quad , \quad (2.1)$$

where j_z and E_z denote the z components of the current density

and the electric field, the z direction being that of the plasma axis. σ is the electric conductivity.

4. Since only relatively low frequencies are applied in the experiment, the real DC component of the so-called AC conductivity [12] can be used and the imaginary conductivity terms are neglected. By restricting ourselves to the DC component we neglect certain time dependences, such as the heating effect connected with the AC modulation. This is justified by the fact that such a heating effect has not been experimentally observed, probably because of insufficient modulation amplitude.

It is thus assumed that

$$\sigma \text{ is real and time independent.}^1 \quad (2.2a)$$

For the radial dependence of the conductivity we use the ansatz

$$\sigma = \sigma_0 [1 - V\hat{r}^2]^P, \quad (2.2b)$$

where $\hat{r} = r/a$ with a the limiter radius. The parameter V allows us to vary the conductivity at the plasma boundary. The conductivity on axis, σ_0 , and the profile number, P , are fitted to conductivity profiles de-

¹Comparison with the transport code of Düchs and McKenney show that the assumption 2.2a is, at least theoretically, not well justified.

duced from Thomson scattering measurements. The parameters σ_0 , V and P have to satisfy additional constraints so that the DC-component of the plasma current, I_{PLO} , equals the experimental value and that the safety factor, q , on axis is of order unity. The DC component, E_0 , of the electric field does not depend on r ; consequently, the plasma direct current is

$$I_{PLO} = 2\pi E_0 \int_0^a dr r \sigma \quad . \quad (2.4)$$

The DC component, E_0 , corresponds to the DC component of the plasma loop voltage

$$V_0 = 2\pi R E_0 \quad , \quad (2.5)$$

where R is the major torus radius. Denoting the DC component of the current density by $j_0(r)$ it follows that

$$j_0(r) = j_0(0) (1 - Vr^2)^P \quad (2.6)$$

with

$$j_0(0) = V_0 \frac{\sigma_0}{2\pi R} \quad . \quad (2.7)$$

Substituting Eq. (2.2b) in Eq. (2.4) yields

$$j_0(0) = (P+1)V \cdot \frac{I_{PLO}}{\pi a^2} \quad (2.8)$$

if the condition

$$(1 - V)^{P+1} \ll 1 \quad (2.9a)$$

is satisfied. The parameters V and P consequently appear in the combination $(P+1) \cdot V$ [for example, in Eq. (2.19)]. It is therefore useful to define the quantity, Q ,

$$Q = (P+1)V - 1 \quad (2.9b)$$

The other constraint is that the safety factor, q , on axis is approximately one. From the definition of q the current density on axis can be shown to be

$$j_o(0) = \frac{2B_{\text{tor}}}{\mu_o q(r=0) R} \quad (2.10)$$

where R is the major radius of the plasma and μ_o the permeability of the vacuum. Inserting this expression into Eq. (2.7), one gets

$$V_o \sigma_o = \frac{4\pi B_{\text{tor}}}{\mu_o q(r=0)} \quad (2.11)$$

Conditions such as $q(r=0) \approx 1$ thus fix j_o and hence the product,

$$V_o \sigma_o \cdot$$

Making use of the simplifying assumptions (1 to 4), a simple parabolic differential equation for the electric field component, E_z , can be derived from Maxwell's equations:

$$\frac{1}{r} \frac{\partial}{\partial r} \left[r \frac{\partial}{\partial r} E_z \right] = \mu_o \sigma \frac{\partial}{\partial t} E_z \quad (2.12)$$

with boundary conditions

$$E_z(r=a) = \frac{V_{PL}}{2\pi R} \quad (2.13)$$

and

$$\frac{\partial}{\partial r} E_z(r=0) = 0 \quad . \quad (2.14)$$

Condition (2.14) assures that the electric field in the plasma center at $r=0$ is continuous. The initial condition at time $t = t_1$ is

$$E_z(r) = \frac{\dot{V}_0}{2\pi R} \quad , \quad (2.15)$$

where V_0 is the DC component of the plasma loop voltage V_{PL} (see Fig. 1b). The parabolic differential equation (2.12 - 2.15) was solved by a numerical method which is described in detail in Section 5.

We now discuss some typical current profiles which were calculated for Pulsator discharges. As will be seen shortly, they can be scaled easily to machines of arbitrary size. With sinusoidal time dependence of the loop voltage, the current density, $j(r,t)$, will also become sinusoidal after a transitional time period of a few cycles; i.e.

$$j(r,t) = j_0(r) + j_1(r) \sin [\omega t + \phi(r)] \quad , \quad (2.16)$$

where the DC component, j_0 , originates from the standard power supply and the AC component, j_1 , from the AC generator and where $\phi(r)$ denotes

the phase with respect to the sinusoidal part of the loop voltage. Some typical examples for the variation of the amplitude of the current density with radius are shown in Fig. 2. We see that the AC current is induced predominantly in the outer layers of the plasma because of the skin effect. On the other hand, only very little current can flow directly at the plasma boundary because the temperature there is low and the resistivity is high. The AC-current density consequently, if ω is sufficiently high, see (2.20), has a maximum at a position, r_{\max} . In order to estimate the position, r_{\max} , of the current-density maximum for tokamaks of arbitrary size with widely differing conductivity profiles, we have derived an approximation formula for r_{\max} obtained from a few dozen examples of our skin effect model

$$\hat{r}_{\max} = \frac{1}{(1+0.135 Q^2)^{0.175} + 2.6 Q \hat{\lambda}} \quad (2.19)$$

In Eq. (2.19), r_{\max} is normalized on the plasma radius and depends on two dimensionless parameters, namely on Q , which was previously discussed in Eq. (2.9b), and on the normalized skin depth, $\hat{\lambda}$,

$$\hat{\lambda} = \frac{1}{a\sqrt{\mu_0 \sigma_0 \omega}} \quad (2.18)$$

Equation (2.19) is valid in the range

$$0.01 \leq \hat{\lambda} \leq 0.2/\sqrt{P} \quad (2.20)$$

$$1 \leq Q \leq 10 \quad (2.21)$$

For $\hat{\lambda} \leq 0.005$ the r_{\max} calculated according to Eq. (2.19) is approximately by 5%^{too} small. For $\hat{\lambda} = 0$ one should get $r_{\max} = 1$, but this limiting case is not correctly reproduced by Eq. (2.19). The RHS of the interval (2.20) describes the case that j_1 is only very slightly larger in the vicinity of r_{\max} than it is for small r . When $\hat{\lambda}$ is further increased, the maximum vanishes and j_1 shows similar qualitative behaviour to the DC profile, j_0 . For $V = 1$ the inaccuracy of the approximation formula is about 0.01 to 0.02. For $V = 0.7$ the r_{\max} calculated according to Eq. (2.19) is already approximately 0.03 too small for $\hat{\lambda} = 0.025$. This effect is caused by the plasma boundary layer, described by V , which was neglected when formulating Eq. (2.19). As soon as $\hat{\lambda}$ becomes larger than the RHS of Eq. (2.20), the AC profile, j_1 , becomes more and more like the DC profile, j_0 , and the subsidiary maximum at r_{\max} vanishes.

The penetration of the alternating current into the plasma depends strongly on the conductivity at the boundary, i.e., in our model on the parameter, V , from Eq. (2.2). Examples of this are shown in Fig. 4. It is found that the AC profile, j_1 , varies more strongly with V than the DC profile, j_0 . It is unfortunate that the conductivity at the boundary is very poorly known experimentally. This causes considerable difficulty in comparing our calculated results with experimental results.

So far only the amplitude of j_1 of the AC current density has been discussed. Because of the phase factor, $\phi(r)$, appearing in Eq. (2.16), the actual time development of the current density profile is slightly more complicated. In Fig. 3 we show the motion of a current density profile during one cycle of the AC modulation using the same conductivity profile as in Fig. 2. The solid line is the DC profile, $j_0(r)$, which represents the current density profile up to the time $t = t_1$. The transient process is not shown in Fig. 3; only the motion after the transition period as described by Eq. (2.16). The motion has a certain vague similarity with the motion of a rope which is tied at the top left and which is under tension and made to oscillate at the bottom right. The waves generated travel from the bottom right to the top left,

their amplitude becomes smaller, till it vanishes at the top left. The wavelength of the oscillation is of the order of the skin depth, $\lambda = 1/\sqrt{\sigma\mu_0\omega}$, at the position, r_{\max} .

The results shown in Figs. 2 to 8 were calculated to match experimental data from the Pulsator experiment, where the minor radius a was 0.11 cm, the central temperature was 0.6 keV, the central conductivity, σ_0 , was $1.4 \cdot 10^7 \Omega^{-1} \text{ m}^{-1}$, and the modulation frequency, ω , in the range $100 \text{ Hz} < \omega < 2000 \text{ Hz}$. Because of the dimensionless formulation of the equations, the figures can be easily scaled to other radii. Consider, e.g., the case $\omega = 1000 \text{ Hz}$ in Fig. 2. For a device with $a = 1 \text{ m}$ and $T_e(0) = 6 \text{ keV}$, the curve would be exactly the same for $\omega = 0.4 \text{ Hz}$, (scaling $\hat{\lambda} = 1/a\sqrt{\mu_0\sigma_0\omega}$). This frequency seems to be very small in comparison with discharge duration and the AC affects only the outermost layer of the plasma.

3. Investigation of Tearing Instabilities

The previous section demonstrated that the radial current density profile can be strongly varied by AC modulation (see, for example, Fig. 3). Since the stability of tearing modes (e.g., Ref. [2]) is strongly dependent on the shape of the current density profile, AC modulation can be used as a powerful tool for the comparison of theoretical predictions of tearing mode theory and experimental observations. This provided the motivation for investigating the AC modulated current density profiles for tearing instability.

The tearing instability develops preferentially at a plasma radius, r_s , where the safety factor, q , is rational;

$$q(r_s) = \frac{m}{n} \quad \text{with } m = 2 \text{ or } 3 \quad (3.1)$$

$$n = 1 \text{ or } 2 \quad .$$

Here m and n are the integer mode numbers of a Fourier expansion in the poloidal and toroidal angles, θ and ϕ . In typical tokamak discharges

$$q(r=0) \approx 1 \quad ,$$

$$q(r=a) \approx 2.3 \text{ to } 8 \quad . \quad (3.3)$$

In order to estimate the stability behaviour, we used a routine, written by Lackner and based on the works of Furth, Rutherford, and Selberg [2] and of White, Monticello, Rosenbluth, and Waddell [3].

This program calculates for a given current density profile, $j_z(r)$, the instability parameters, Δ' , r_s , and w , the significance of which is explained as follows:

1) Δ' is the jump of the logarithmic derivative of the eigenfunction of the mode at the resonant q -surface and determines the linear growth rate, γ . The relations between Δ' and γ was first described by Furth, Killeen, and Rosenbluth [1]. A nice representation is given in Batemans monograph [4] which gives [Eq. (10.2.20)]

$$\gamma = 0.55 \Delta'^{0.8} \eta^{0.6} (kB'_*)^{0.4} \rho^{-0.2} \quad , \quad (3.4)$$

where η is the resistivity, ρ the plasma density, and B the magnetic field strength.

Δ' also determines the marginal instability. According to Furth, Rutherford, Selberg [2], for a cylindrical zeropressure plasma, the instability criterion is

$$\Delta' > 0 \quad . \quad (3.5)$$

Glasser, Johnson, and Greene [5] have also taken the pressure and toroidal effects into account. Instead of Eq. (3.5), they obtain the criterion for marginal instability

$$\Delta' > \Delta_{\text{crit}} \quad . \quad (3.6)$$

In typical tokamak discharges one obtains a small improvement of the stability, i.e.,

$$a \Delta_{\text{crit}} \approx 1 \text{ to } 3 . \quad (3.7)$$

2) r_s is the radius of resonant q surface.

3) w is the (full) width of the saturated magnetic island associated with the tearing mode; the island width normalized to the plasma radius is defined as \hat{w} , where

$$\hat{w} = w/a . \quad (3.7a)$$

The island width, w , depends on the nonlinear saturation amplitude of the tearing mode. According to White, Monticello, et al. [3], island formation leads to flattening of the current profile in the vicinity of the resonant q surface. The island continues to grow until one has $\Delta' = 0$ for the flattened current profile. The nonlinear saturation width of the island can be estimated according to Jaenicke, Wobig, and Callen [9,16] in a very rough approximation by calculating the value w for which

$$\frac{\partial}{\partial r} \left[\psi_1 \left(r_s + \frac{w}{2} \right) - \psi_1 \left(r_s - \frac{w}{2} \right) \right] = 0 , \quad (3.8)$$

where $\psi_1(r)$ is the radial part of the linear eigenfunction of the mode expressed in terms of the helical flux,

$$\psi = \psi_0(r) + \psi_1(r) \cos(m\theta + n\phi) . \quad (3.9)$$

According to the present view a magnetic island grows until its width

attains the value, w . If it then overlaps an adjacent island, there is ergodization of the magnetic field lines near the islands. This leads to disruption of the magnetic confinement of the plasma [6,7]. Overlapping of the $m = 2, n = 1$ mode with the $m = 3, n = 2$ mode appears to be particularly dangerous.

We now discuss some typical results of these calculations. First, we investigate the stability of the DC profile. For typical Pulsator current profiles the $m = 2, n = 1$ mode is marginally unstable while the higher m modes are stable. For example, for the profile

$$j_o = 7 \cdot 10^6 (1 - 0.716 r^2)^{5.76} \quad (3.10)$$

values of $a\Delta'$ listed in Table I are obtained.

TABLE I

m	n	$a\Delta'$
2	1	4.3
3	2	- 1.5
3	1	- 4.5
4	1	- 7.4
4	2	- 8.0
4	3	- 8.4
5	1	- 9.1
5	2	-11.0
5	3	-13.0
5	4	-16.0

If AC modulation is applied, the DC current density as well as $d/dr j_z$ at the resonance surface, and hence Δ' , will vary periodically. According to the instability criterion, $\Delta' > \Delta'_{crit}$, the modes therefore become unstable with increasing AC amplitude in the sequence given in Table I. Figure 5 shows an example of a sinusoidal AC modulation. This figure was obtained with the ordinary differential equation (7.2) (see Sec. 7 on the GOEL program). Using the partial differential equation (2.12) to (2.15) and plotting Δ' for the 7th cycle, one obtains Δ' values approximately 20% lower than the corresponding Δ' values of Fig. 5, indicating that the relaxed state has not yet been completely attained after 7 cycles. Unlike Fig. 5, Figs. 6,7 and 8 were calculated according to Eq. (2.12) to Eq. (2.15).

For low amplitudes the modulation of Δ' is sinusoidal (e.g., the curve $\Delta I = 5$ kA in Fig. 5). For high amplitudes, on the other hand, Δ' is not sinusoidal (e.g., $\Delta I = 20$ kA in Fig. 5). This non-sinusoidal modulation of Δ' is due in part to the strong radial motion of the resonant surface. As a consequence, the mean value $\langle \Delta' \rangle$, i.e., Δ' averaged over a cycle of the AC modulation, increases strongly with the AC voltage, indicating that the plasma is destabilized. This behaviour was found typical for all sinusoidal AC modulations.

Figure 6 shows examples in which the frequency was varied. For higher frequencies and comparable current modulation the mode 3/1 becomes unstable (see Fig. 6b). At even higher frequency, the 4/1 mode is destabilized, so that AC heating of the plasma boundary layers is likely to be difficult.

The physical interpretation of the quantity, Δ' , and its mean value, $\langle \Delta' \rangle$, should now be further discussed. As shown previously, $\Delta' > \Delta_{\text{crit}}$ corresponds to instability [see Eq. (3.6)], and Δ' determines the linear growth rate [see Eq. (3.4)]. It is also known [13] that the range of validity of the linear theory is restricted to very low amplitudes. For somewhat higher amplitudes the modes grow according to Rutherford's formula [13]

$$\frac{d\hat{w}}{dt} \equiv \frac{\hat{w}}{t_i} = \frac{1.66}{\sigma \mu_0 a^2} \Delta' (w=0) \quad . \quad (3.12)$$

Even this reduced growth rate, t_i , is, in most cases, much smaller than the period, t_{AC} , of the AC modulation:

$$t_i \ll t_{\text{AC}} \quad . \quad (3.13)$$

In the case of Fig. 5a, for example, one has

$$t_A = \frac{2\pi}{\omega} = 2.5 \text{ ms},$$

$$t_i = 0.6\sigma\mu_0 a^2 w/\Delta' = 0.1 \text{ to } 0.2 \text{ ms},$$

where $\sigma = 0.2 \times 10^7$ (ohm⁻¹ m⁻¹) at the resonance surface,

$$\mu_0 = 4\pi \cdot 10^{-7} \text{ (V s A}^{-1} \text{ m}^{-1}\text{) ,}$$

$$a\Delta' = 14 \text{ (for } \Delta I = 10 \text{ kA),}$$

$$a = 0.11 \text{ m ,}$$

$$\hat{w} = 0.1$$

Consequently, as soon as a mode has become unstable, the saturation amplitude is very quickly attained - if condition (3.13) is satisfied -, and the magnetic islands develop almost immediately to their full width.

It is therefore of interest to discuss the behaviour of the island width w . First, there is no direct connection between w and Δ' . If Δ' is negative, the plasma is stable with $w = 0$, but as soon as Δ' becomes positive a magnetic island of finite width, w , forms. In our calculations, however, we have found both large w together with small Δ' and, conversely, small w with large Δ' . It therefore seems advisable to discuss the behaviour of w from examples.

Figure 7 shows the position, \hat{r}_s , of the resonant surface and the curves, $\hat{r}_s + w/2$ plotted versus "time", t , for typical Pulsator conditions. Without AC modulation the mode $m/n = 2/1$ is unstable at all times and an island with normalized width, $\hat{w} \cong 0.2$, forms. The island width becomes slightly modulated by a small AC current ($\Delta I = 3.5$ kA, Fig. 7a). For larger AC modulation ($\Delta I = 5.2$ kA, Fig. 7b) Δ' becomes negative for a short time so that the island vanishes. At other time phases the $3/2$ mode also becomes unstable. With even larger AC modulation ($\Delta I = 10$ kA, Fig. 7c) the islands of the $2/1$ and $3/2$ modes overlap. This overlapping is caused, among other things, by the fact that the resonant surfaces approach each other closely during the time phase in which the two modes are unstable and simultaneously have large islands. Our model thus predicts that at certain time phases stabilization of the $2/1$ mode will occur and that at other time phases the $2/1$ and $3/2$ modes overlap. It should be possible

to verify these predictions experimentally because the Mirnov oscillations should vanish during the stabilized phase and disruptions should occur during the overlapping phase.

In summary, it can be stated that AC modulation varies periodically the current profile, and hence the stability of the plasma periodically improves and deteriorates. The stability depends on a series of factors e.g., the motion of the resonant surfaces, the steepness of the current density profile and many others. With sinusoidal modulation these factors generally tend to cause a deterioration of the stability properties. It was hoped, however, that the most unfavourable effects will be minimized by appropriate non-sinusoidal modulation. We therefore investigated numerous non-sinusoidal modulations. We can summarize the most important results: with carefully tailored sawtooth modulation of the current (see Fig. 8a) overlapping of the magnetic islands of various modes did occur at much higher amplitudes, ΔI , than for comparable sinusoidal modulation. To obtain this result, we introduced short voltage pulses at regular time intervals, $2\pi/\omega$, for the AC component of the plasma loop voltage, V_{PL} . Between two voltage pulses we kept V_{PL} constant. These voltage spikes (Fig. 8a, curve V_{PL}) lead to a sawtooth-like current modulation (Fig. 8a, curve I_{PL}). In Fig. 8 the amplitude of the voltage pulses is chosen such that the amplitude, ΔI , of the current modulation is the same as that in Figs. 6a and 7c for sinusoidal modulation. Comparison of the two cases shows that:

- 1) The mean value $\langle \Delta' \rangle$ is about 6.2 in both cases, irrespective of the shape of the current modulation.
- 2) With sinusoidal AC modulation (Fig. 7c) overlapping of the magnetic islands occurs; with the sawtooth modulation of the current chosen in Fig. 8 there is no overlapping.

There is no "genuine" stabilization involved in this case since $\langle \Delta' \rangle$ is roughly as large as in the comparable sinusoidal case, but overlapping is prevented because of the larger separation of the resonant surfaces during the unstable phase compared with the sinusoidal case.

The opposite case that $\langle \Delta' \rangle$ is reduced can also be obtained by applying negative voltage pulses and an inverted sawtooth modulation of the current [15]. In this case, however, overlapping occurs for much smaller amplitudes than for sinusoidal modulation.

While we could improve the stability properties compared to sinusoidal modulation, we have found no case where the stability was improved over the DC case, considering both the $\langle \Delta' \rangle$ criterion and the overlapping criterion.

4. Heating Power

Finally, we want to discuss the heating effects associated with AC-modulation. The primary motivation for this investigation has been to check, whether the absence of heating effects in the Pulsator experiment is consistent with the prediction of our model. Due to the skin effect the AC will preferentially heat the outside of the plasma column. The AC heating competes with the DC-input energy which is transported through the outside region. We therefore took as a criterion that the AC heating power has to be comparable with a reasonable fraction of the DC power input in order to have a noticeable effect.

First, we study how the heating power depends on the parameters. In our model the total heating power, averaged over a cycle, is

$$\langle H \rangle = \frac{1}{2\pi} \int_0^{2\pi} d(\omega t) 4\pi^2 R \int_0^a dr r \sigma E_z^2 . \quad (4.1)$$

With sinusoidal modulation one has

$$E_z = E_0 + E_1 \cos(\omega t + \phi) , \quad (4.2)$$

where E_1 and ϕ depend on r . The DC component, E_0 , depends neither on space nor time. We can therefore divide the heating power into a DC component, H_0 , and an AC component, H_1 :

$$\langle H \rangle = H_0 + H_1 , \quad (4.3)$$

where

$$H_1 = 2\pi R \int_0^a dr r \sigma E_1^2 \quad (4.4)$$

$$H_1 \approx 2\pi R a^2 E_1^2(a) \hat{\lambda}^x \quad (4.6)$$

$$x = 1.213 + 0.34 \ln Q \quad (4.7)$$

The two parameters, $\hat{\lambda}$ and Q , have already been introduced in Eqs. (2.9b) and (2.18); they are the "essential" parameters of the problem. The approximation formula (4.6) was obtained from a several examples, the inaccuracy being approximately 10%. Equations (4.2 to 4.7) are only valid in the relaxed state. It should be mentioned that this state is reached often only after many cycles and that the heating power, H_1 , depends very sensitively on how exactly the relaxed state is attained. In the example in Fig. 7b, H_1 in the 7th period is about 9 kW, but in the 37th period is about 5 kW. The latter value corresponds very well to the relaxed state.

The amplitude of the AC modulation and consequently also the AC-heating power is limited by the development of instabilities, which can lead to disruptions. In our model this is equivalent to the overlapping of two islands of different helicities. We therefore have investigated at what AC amplitudes the islands come into contact with each other and what heating power corresponds to these AC amplitudes. In the example shown in Fig. 7b, the DC-power input is 120 kW, while the AC power is 5 kW. Moreover, Fig. 7b shows that the 3/2 and 2/1 islands are so close that the AC-power input is at its upper limit. This and similar calculations showed that for sinusoidal AC modulation the maximum ratio H_1/H_0 is only a few percent. This result is in good agreement with the experiment.

We mention that for higher frequencies a larger value for the ration

H_1/H_0 can be obtained without overlap. For instance, for the same parameters as in Fig. 7b, but with $\omega/2\pi = 10^4$ Hz, we obtain $H_1 \approx H_0$. In this case the heating power input is limited because the 3/1 and the 4/1 mode overlap. At the high frequencies, however, it is only the extreme outer plasma boundary layer that is heated by the AC-modification and the energy confinement in this layer is very short.

Finally, we obtained considerably larger values of H_1 with sawtooth modulation. This is due to the prevention of overlapping as discussed in Sec. 3. In the example shown in Fig. 8, overlap does not happen until $H_1/H_0 \geq 20\%$, i.e., more than twice the value of a comparable sinusoidal modulation (Fig. 7b). But even in this more favorable case, the heating effects probably would be only marginally observable in our experiment.

Before we proceed with a detailed description of the computer programs, we want to summarize the main conclusion of our computation regarding the physics of the AC-modulation.

(a) Through AC modulation the current density profile in tokamak plasmas can be quite significantly altered, which in turn significantly modifies the stability of tearing modes. One of the surprising features of the experiments [14,15] has been the fact that ^{relative} ~~very~~ large AC amplitudes could be applied without disrupting the plasma. The computations showed that although the instability parameter, Δ' , may become very large, ($\Delta' \approx 10-15$), overlap of islands does not necessarily occur. The AC amplitudes which are needed to produce overlap are - according to our computations - comparable to the experimentally observed amplitudes.

(b) Overlap should occur when the saturation width, w , of the island becomes very large and when the distance between resonant surfaces becomes small. Both factors seem to be of equal importance. By suitable shaping of the applied AC-voltage, e.g., by applying a sawtooth shaped current modulation rather than sinusoidal one, we were able to move resonance surface apart during the unstable period of the AC modulation.

This method can reduce some of the adverse effects of sinusoidal AC-modulation. However, we were not able to obtain better stability than with the DC-current profile.

(c) The calculations predict that disruptions caused by changes in the current density profile during AC occur before significant heating is produced by the AC-modulation. The best heating efficiency was obtained by sawtooth modulation, and the AC power input was about 20% of the DC power input.

FIG. 1a

Scheme of experimental arrangement

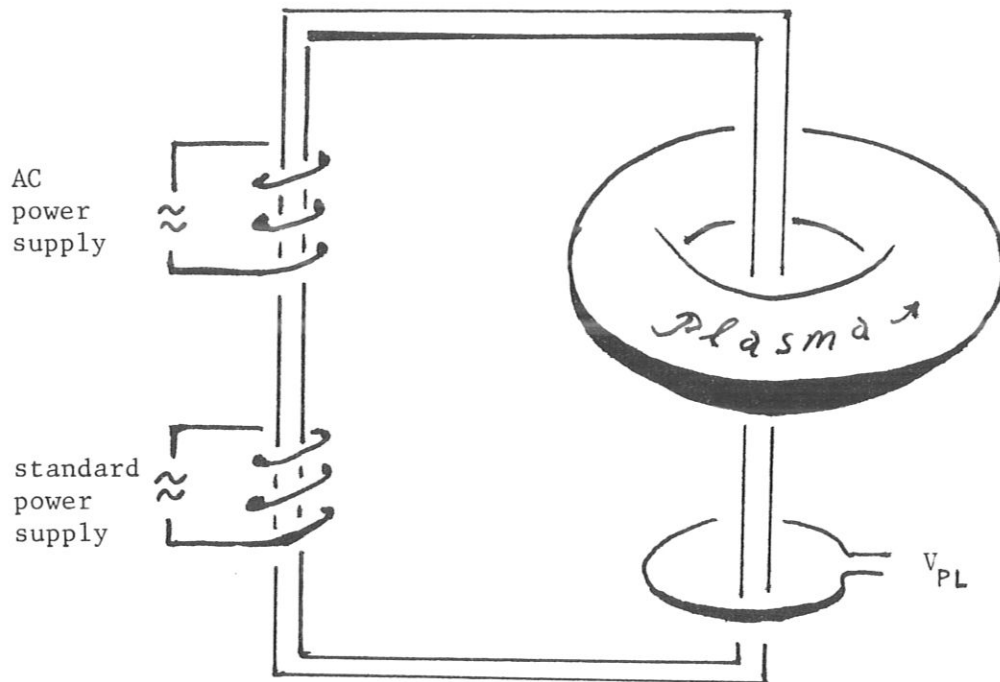


FIG. 1b

Plasma current I_{PL} and loop voltage V_{PL}
versus time t

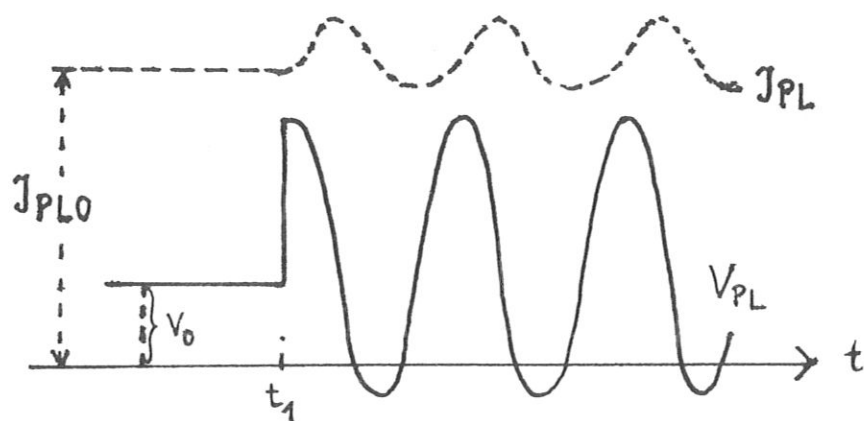


FIG. 2

Current Densities, j_0 (= DC) and j_1 (= AC) normalized on 1, versus $\hat{r} = r/a$, for

$$\sigma = 1.4 \times 10^7 [1 - 0,716 \hat{r}^2]^{5.76} [\text{Ohm m}]^{-1}$$

$$\frac{\omega}{2\pi} = 100 ; 300 ; 1000 \text{ sec}^{-1}$$

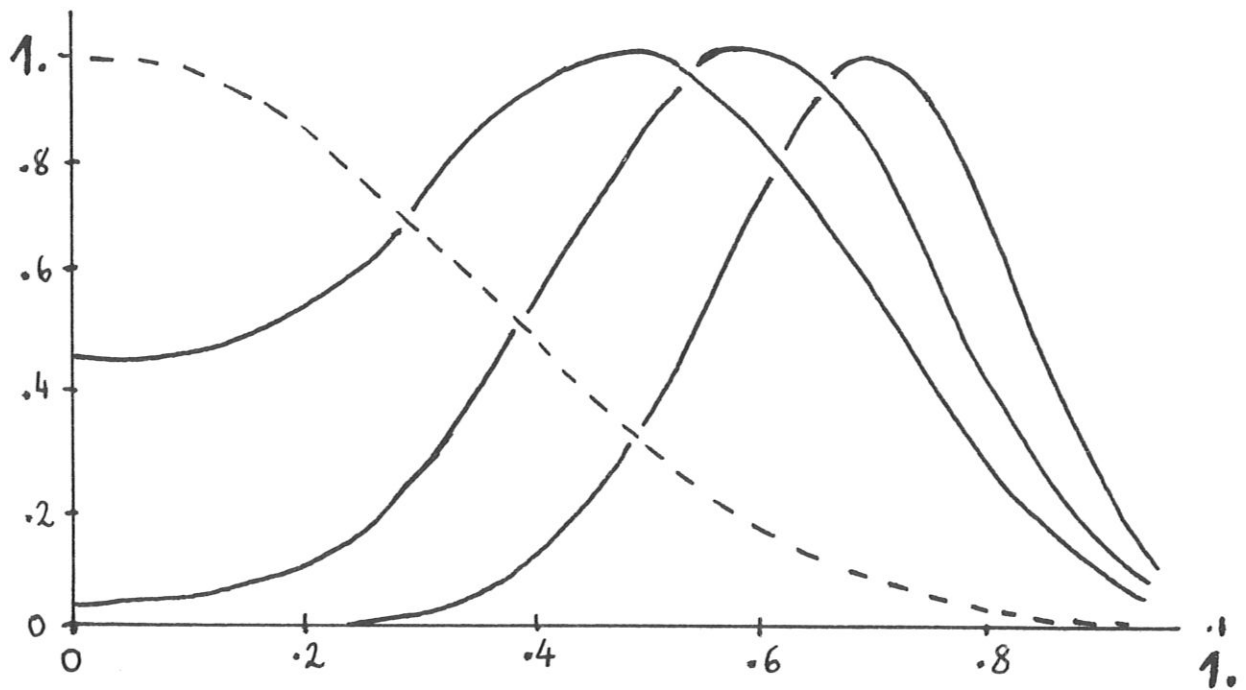


FIG. 3

Current Density Distribution during AC-Modulation

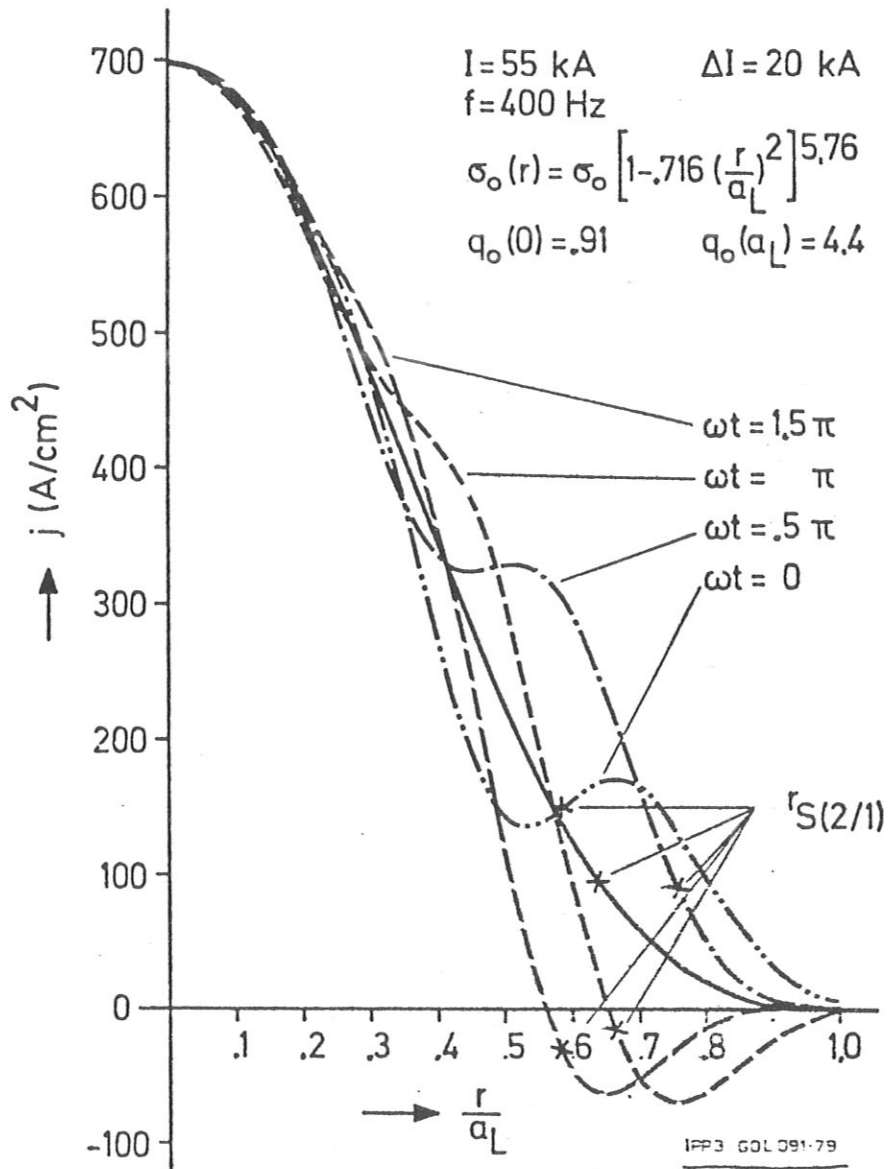


FIG. 4

Current densities j_0 (= DC) and j_1 (= AC) versus $\hat{r} = r/a$, for

$$\sigma_1 = 1.4 \times 10^7 [1. - 1. \hat{r}^2]^{3.85} \text{ [Ohm m]}^{-1}$$

$$\sigma_2 = 1.4 \times 10^7 [1. - 0.716 \hat{r}^2]^{5.76} \text{ [Ohm m]}^{-1} \quad (\hat{r} \geq 0.7)$$

$$\sigma_3 = 1.4 \times 10^7 [1. - 0.2 \hat{r}^2]^{23.2} \text{ [Ohm m]}^{-1} \quad (\text{dashed})$$

$$V_0 = 2.2 \text{ Volt}$$

$$V_C = 50. \text{ Volt}$$

$$\frac{\omega}{2\pi} = 300 \text{ sec}^{-1}$$

$$I_{PL} = 55 \text{ kA}$$

$$\text{Note: } V_{PL} = V_0 + V_C \cos \omega t.$$

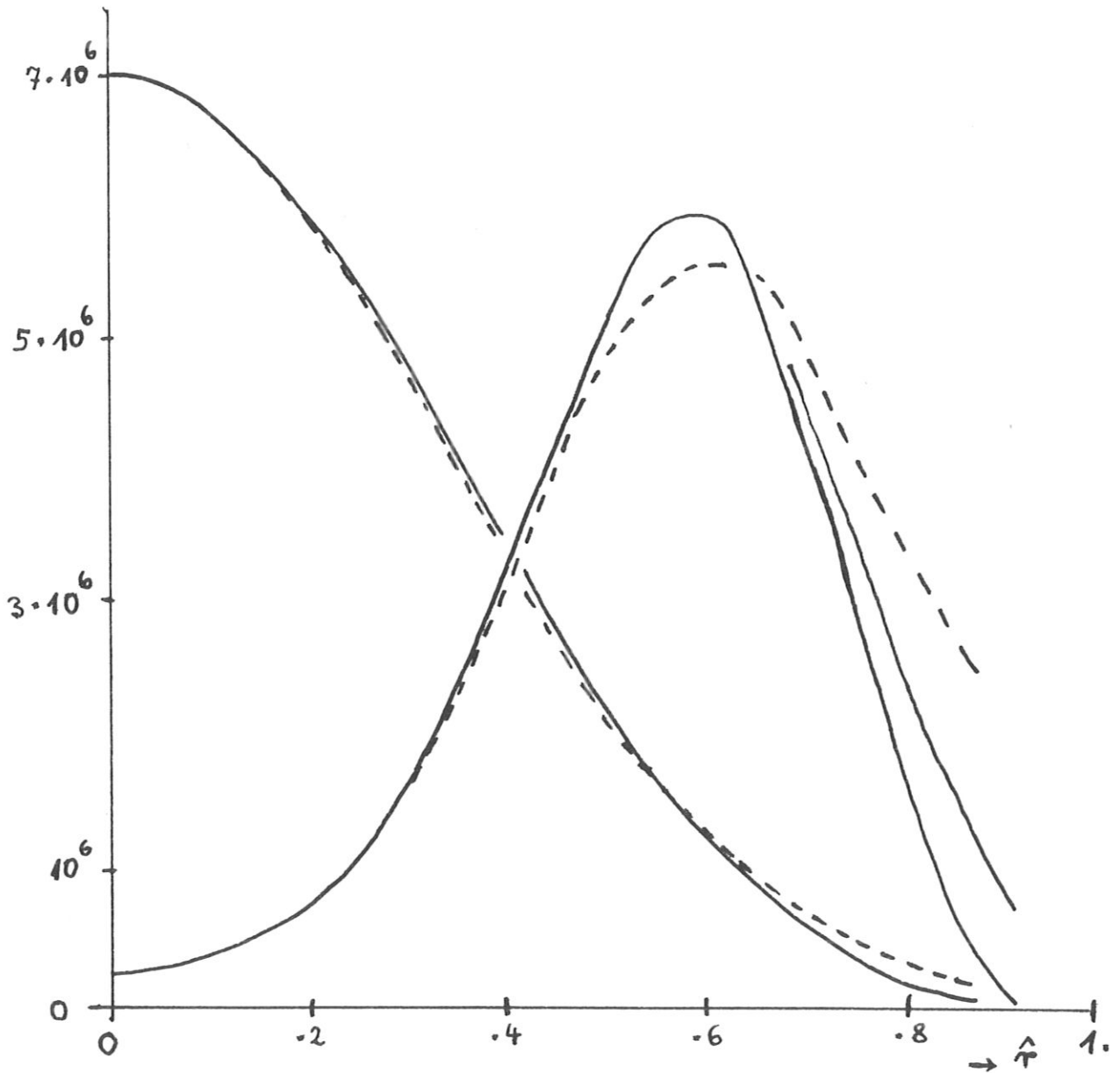


FIG. 5

$\partial \Delta'$ versus ωt for $I_{PL} = 55. \text{kA}$

$\frac{\omega}{2\pi} = f = 400 \text{ sec}^{-1}$

$j_o(r) = 7 \times 10^6 (1. + 0.716 \hat{r}^2)^{5.76} [\text{A m}^{-2}]$

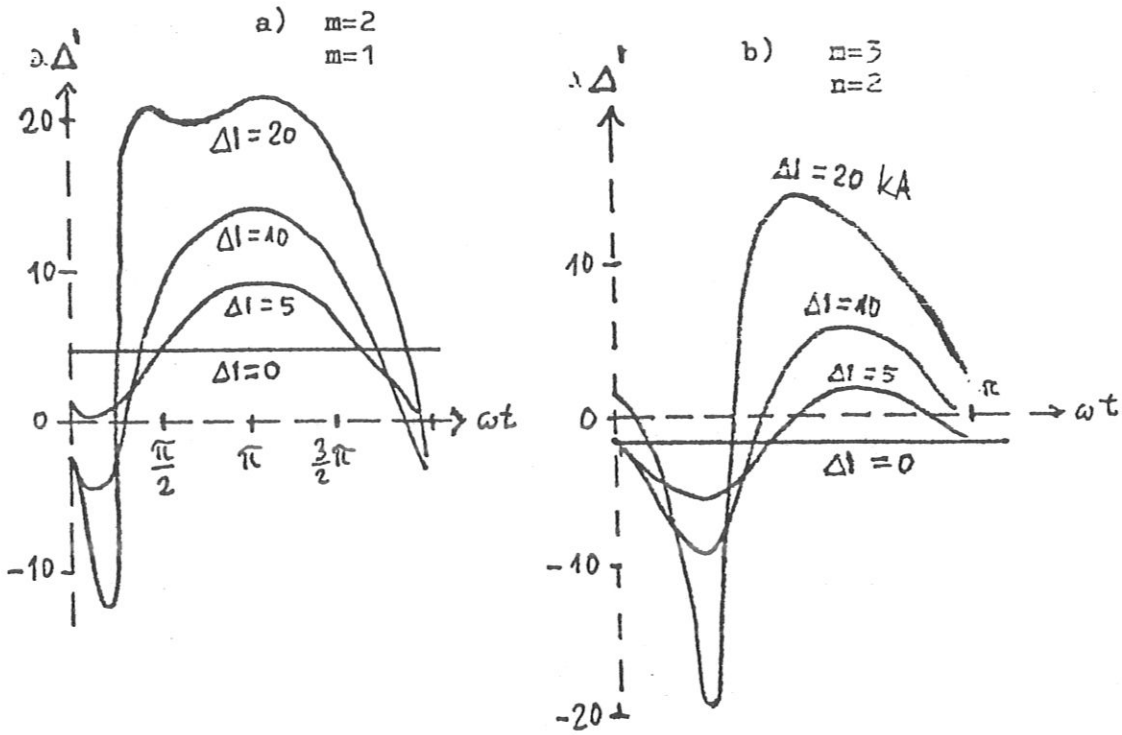


FIG. 6

$\partial \Delta'$ versus ωt for $I_{PLO} = 55. \text{kA}$ and $j_o(r)$ from FIG.5 calculated from eq.(2.12 for the 7th cycle

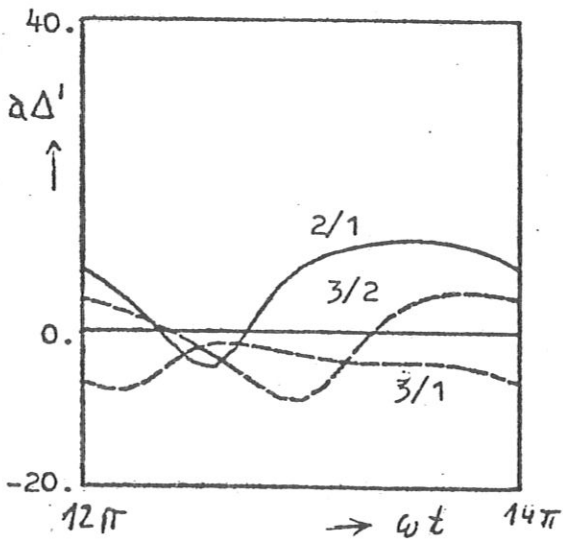


FIG.6a

$\frac{\omega}{2\pi} = 400. \text{sec}^{-1}$ (vgl. FIG.5)

$\Delta I = 10. \text{kA}$

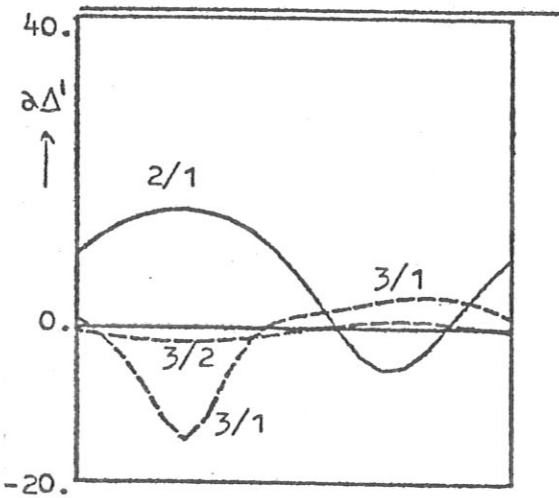


FIG.6b

$\frac{\omega}{2\pi} = 4000. \text{sec}^{-1}$

$\Delta I = 8. \text{kA}$

FIG. 7

\hat{r}_s , $\hat{r}_s + \frac{\hat{w}}{2}$ und $\hat{r}_s - \frac{\hat{w}}{2}$ versus ωt

for three values of the current modulation ΔI .

\hat{r}_s = radius of the resonant q surface,

\hat{w} = full width of the magnetic island,

\hat{r}_s and \hat{w} are normalized to the plasma radius.

The other parameters are the same as in FIG. 6a.

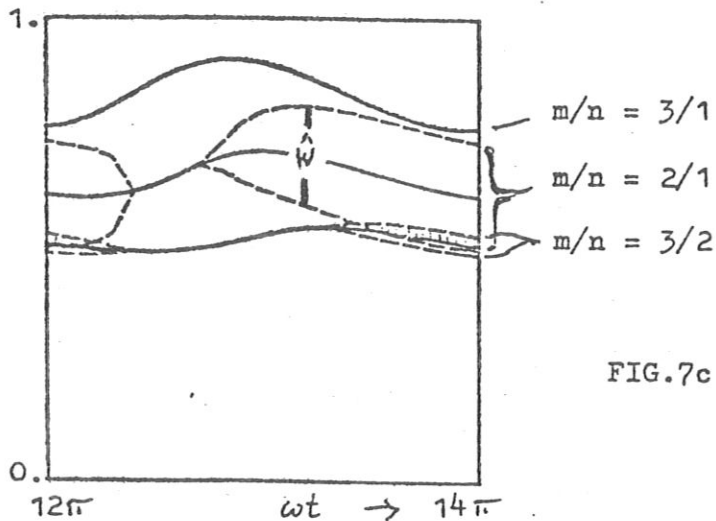
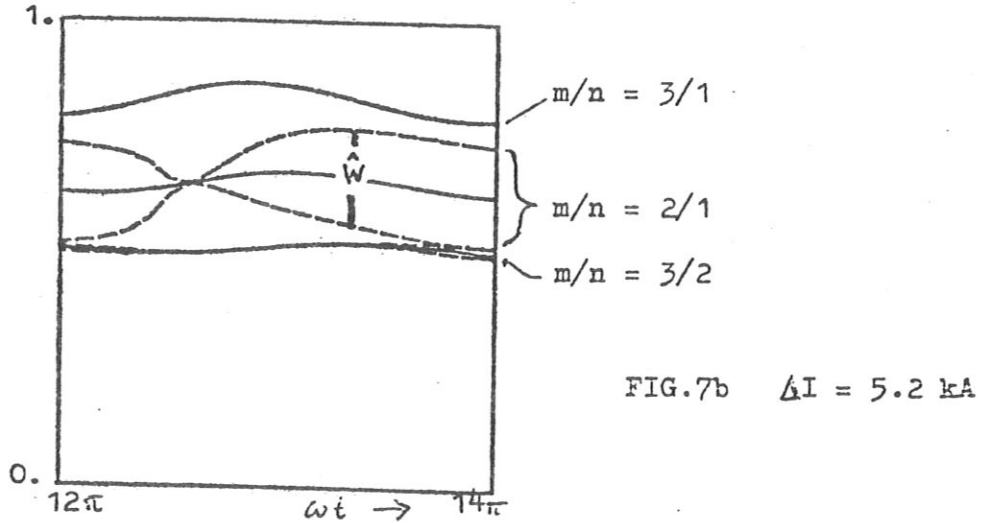
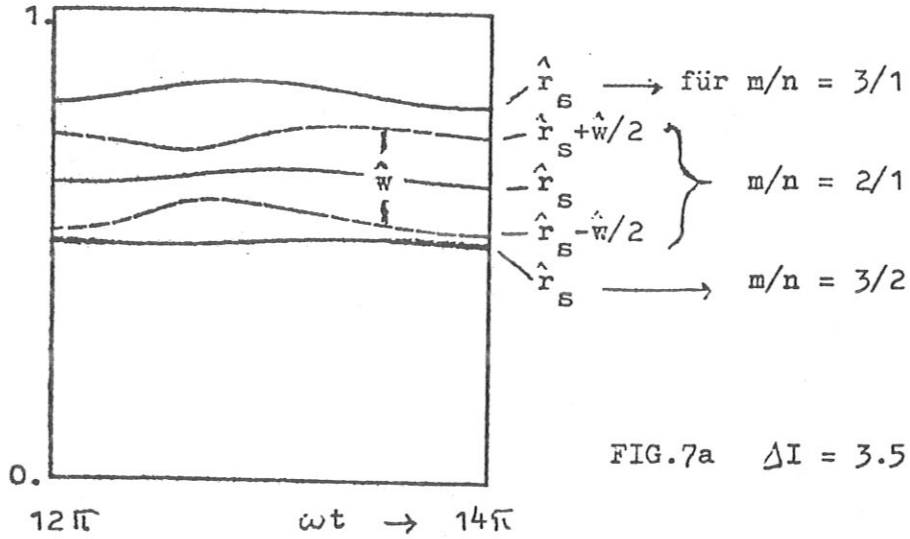


FIG. 8

Sawtooth modulation of the plasma current.

All parameters are the same as those in FIGS. 6a and 7c.

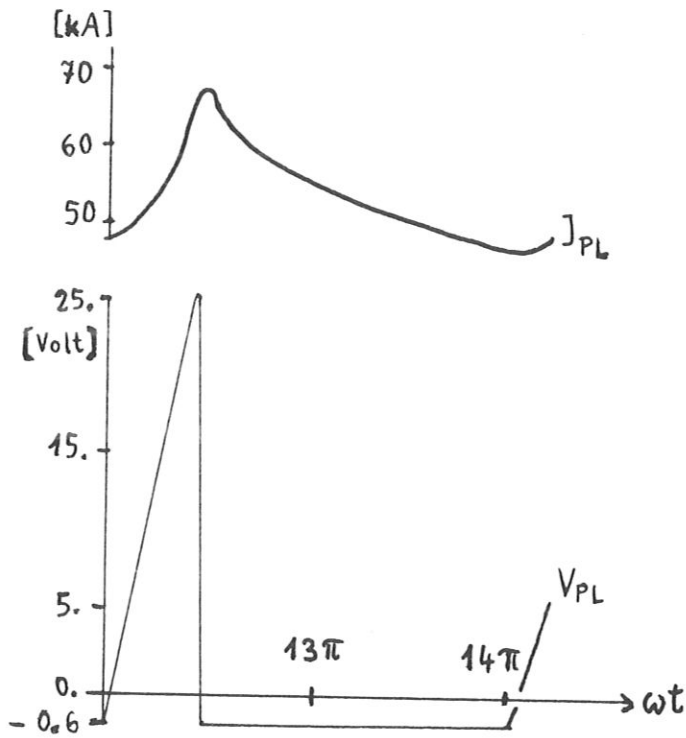


Fig. 8a
 plasma current I_{PL} and
 loop voltage V_{PL}
 versus ωt .
 The amplitude of the
 current modulation is
 $\Delta I = 10$. kA.

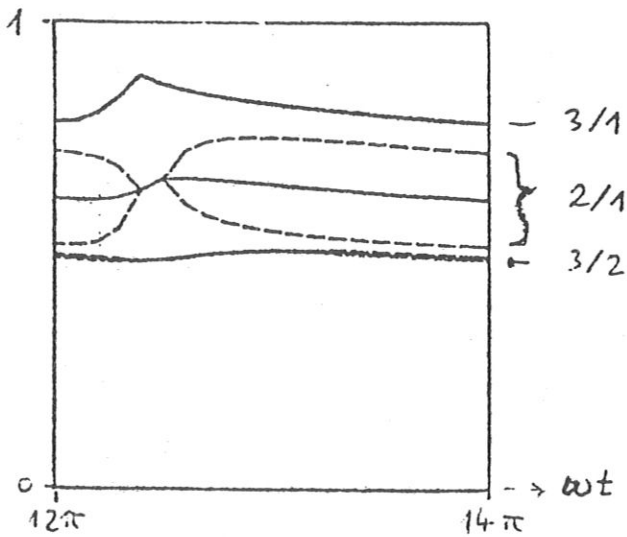


FIG. 8b
 $\hat{r}_s, \hat{r}_s = \frac{\hat{w}}{2}$ und $\hat{r}_s - \frac{\hat{w}}{2}$
 versus ωt .

APPENDIX: Computer programs

5. GEOPAR program

The figures shown in sec. 3 are calculated with the GEOPAR program. This program is now described in detail to allow the reader to reproduce these figures or to produce similar figures with other parameters. The program has the following objectives:

- 1) input and preparation of necessary parameters;
- 2) Calculation of
 - radial mesh points,
 - conductivity,
 - initial conditions for the field component E_z ,
 - shape factor COSOMZ determining modulation,
 - current density profile,
 - heating power,
 - instability parameters (from FURTH subroutine),
 - E_z at equidistant time intervals (from PARCYL subroutine)
- 3) drawing of figures in the ZEICH subroutine; for this purpose the quantities of interest are stored in the two-dimensional array Z at the end of the SIGFRI subroutine.

1) Meaning of input parameters

We start with the integer parameters:

M(J) and N(J) are the mode parameters, i.e. the wave numbers of a Fourier expansion of the helical flux in the poloidal angle and toroidal angle; see table below in the section of SIGFRI;

NPR(J) the times at which current profiles and instability parameters should be calculated, in units of the time step size DT defined below.

Such a parameter array is necessary because,
 on the one hand, DT has to be fairly small for numerical
 calculation of E_z , and,
 on the other, current profiles and instability para-
 meters are only needed after relatively large time intervals;

LMA = number of radial mesh points;
 NP = number of AC cycles;
 NT = number of time intervals per cycle.

The real parameters are now given in alphabetic order:

A = radius for which the profile function for the conductivity
 vanishes (in metres); (*see FIG.9*);
 AL = limiter radius = a (*in metres*)
 the connection with parameter V from eq.(2.2) is explained below;
 BTOR = toroidal field in tesla (1 tesla = 10^4 gauss);
 FR = AC frequency in $s^{-1} = \frac{\omega}{2\pi}$
 P = profile number from eq. (2.2)
 RG = major radius in metres;
 SIGO = σ_0 from eq. (2.2);
 V_C = AC voltage in volts;
 V_G = DC voltage in volts;
 R_{SOND} = distance of sond from the plasma axis, this parameter is
 not used in this paper.

Other parameters

DR = space step = AL / (LMA - 1);
 DT = time step = 1 / (FR NT) = $2\pi / (\omega NT)$ [s];
 MO = μ_0 from eq. (2.10) = $4\pi \cdot 10^{-7}$ in units $[\frac{Vs}{Am}]$;

Q_F = time independent component of the safety factor q .

For q the following equations are valid:

$$q = \frac{r B_{\text{tor}}}{R B_{\text{pol}}} = \frac{2\pi B_{\text{tor}}}{\mu_0 R} \frac{r^2}{I(r)}, \quad (5.1)$$

where $Q_F = \frac{2\pi B_{\text{tor}}}{\mu_0 R}$ is the space and time independent component of q .

and
$$I(r) = 2\pi \int_0^r dr' r' j_z(r') \quad (5.2)$$

$I(r=a)$ is thus equal to the plasma current I_{PL} .

$$\text{VERS} = \left[\frac{A_L}{A} \right]^2 = V \text{ from eq. (2.2).}$$

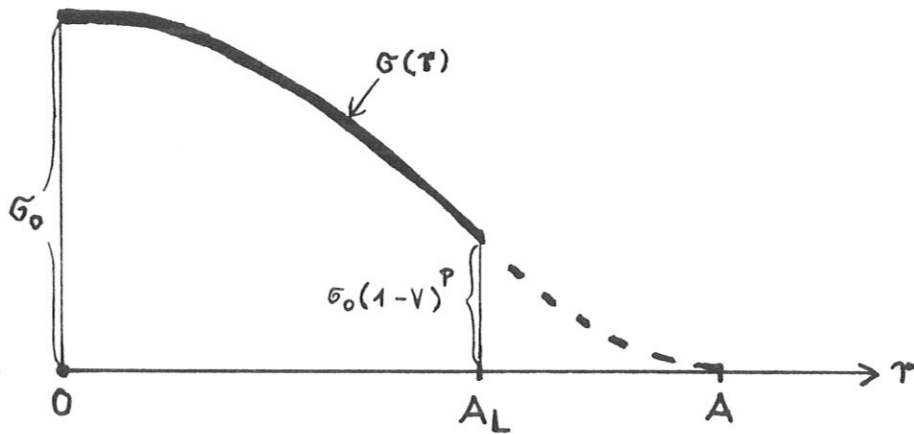


FIG. 9

illustrates the

significance of A_L and A and V .

2) COSOMZ

The plasma loop voltage is periodic for $t \geq t_1$. We write in the form

$$V_{PL} = V_G + V_C \text{COSOMZ}.$$

This equation is also valid for $E_z(a)$ because of eq. (2.13). With sinusoidal AC modulation one has according to eq. (2.16):

$$\text{COSOMZ} = \cos \omega t;$$

hence the name COSOMZ. The AC voltage does not, however, have to be sinusoidal; it may also be sawtooth-like or otherwise. The FORM subroutine calculates COSOMZ for one cycle, i.e. for $J = 1$ to $J = NT$. Meanwhile there are many such FORM subroutines which are stored in various AMOS segments, e.g. sinusoidal modulation in FORM6;
 sawtooth modulation in FORM2;
 etc.

3) SIGFRI

The SIGFRI subroutine calculates for a given field $E_z(r)$:

the current density profile $j_z(r)$

the heating power $\int dr r E_z(r) j_z(r) 4\pi^2 R/1000$ [kW]

and, by means of CALL FURTH, the instability parameters

$$D_L(K) = \Delta' a,$$

RQ(K) = radius of the resonant Q surface, divided by a

and DE(K) = half island width = $\frac{\hat{w}}{2}$.

Here the index K gives the number of pairs of mode parameters m, n which have to be taken into account. In the curves shown in this report these are:

K	m	n
1	3	1
2	3	2
3	2	1

SIGFRI is called at two points:

- 1) as soon as the initial values for E_z are available;
- 2) in the DO-7 loop after CALL PARCYL for the values of E_z calculated by PARCYL; but, of course, only for those times NPR(LS) for which the current density and instability parameters are to be calculated; hence the inquiry in statement ISN 0046 in the main program.

We require various radial mesh point distributions because:

In the FURTH subroutine

the index $L = 1$ has to be assigned the value $\hat{r} = 0$ and

the index $L = LMA$ has to be assigned the value $\hat{r} = 1$;

the plasma radius thus has to be normalized to 1.

In the PARCYL subroutine

the value $r = 0$ has to be in the centre between $L = 1$ and $L = 2$

the value $r = a$ has to be in the centre between $L = LMA$ and $LMA-1$;

$R(L = 1)$ is thus negative.

The parameter JWRITE regulates the printout of the results:

with $JWRITE = 0$ nothing is printed out,

with $JWRITE \geq 2$ ZEIT, current profile, q etc. are printed out.

After calculation of the current profile CALL FURTH is given for calculating the tearing instability parameters; the quantities of interest are stored in array Z.

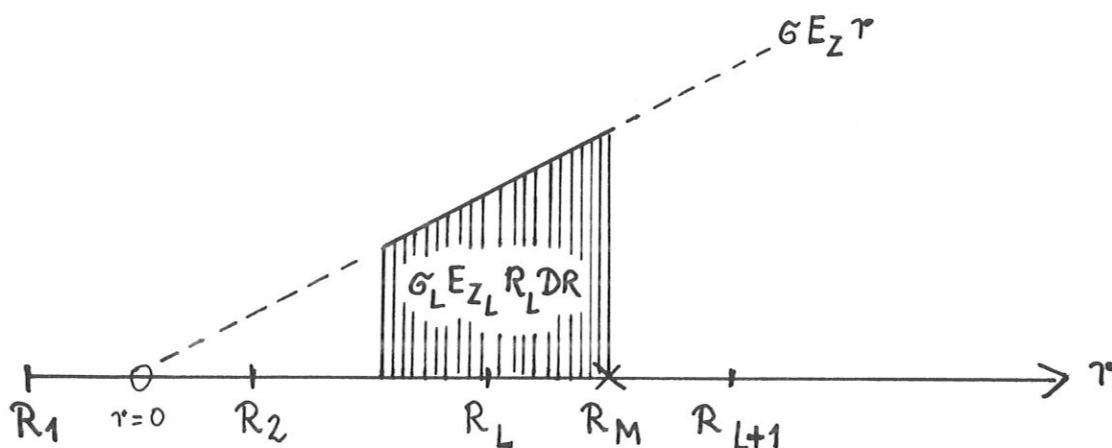


FIG. 10 For SIGFRI subroutine, DO-5 loop

Figure 10 shows the positions of the R mesh points which are needed for PARCYL, with R_1 negative. The hatched surface illustrates the calculation of the current, which with equidistant R_L is as follows:

$$I(R_M) = 2\pi \int_0^{R_M} dr r \sigma(r) E_Z(r)$$

$$\approx I_R = 2\pi DR \sum_{L'=2}^L R_{L'} \text{SIG}_{L'} E_{Z_{L'}}$$

6. PARCYL subroutine

The name stands for PARAbolic partial differential equation with CYLindrical symmetry. The PARCYL subroutine calculates

$$E_Z \text{ at time } t + DT$$

from E_Z at time t .

We now describe the numerical method by which this is done.

Given is the parabolic partial differential equation

$$\frac{1}{r} \frac{\partial}{\partial r} \left[r \frac{\partial F}{\partial r} \right] = S \frac{\partial F}{\partial t}$$

with the

boundary conditions $\frac{\partial F}{\partial r} = 0$ for $r = 0$,

$$F = G$$
 for $r = a$.

$G = G(t)$ and $S = S(r,t)$ are given functions.

Required $F = F(r,t)$.

In order to solve the equation numerically we approximate the given differential equation by a difference equation. For this purpose we introduce equidistant time mesh points and space mesh points r_j ; the r_j need not be equidistant. The point $r_j = 0$ has to be left out because of the factor $\frac{1}{r}$ in the given differential equation. Let

$$F_j = F(r_j, t)$$

and

$$\hat{F}_j = F(r_j, t+DT).$$

The F_j are known, either as initial values or from the previous time step; the \hat{F}_j are to be calculated from the F_j . The difference equation can be divided into recursion formulae, which are solved successively from the boundary conditions.

First we present the discretization scheme and then the formulation and rearrangement of the difference equation.

Discretization scheme

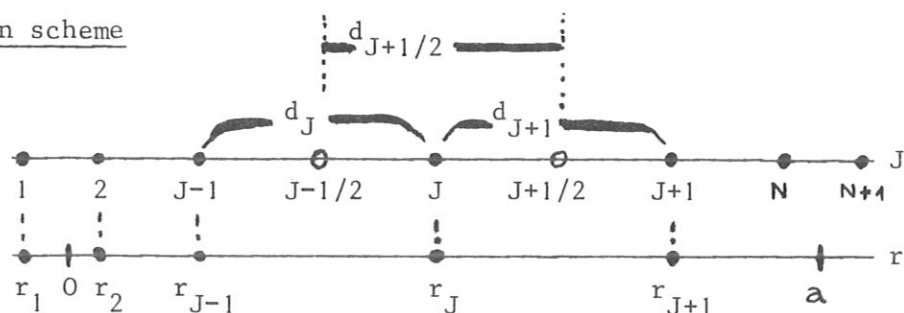


FIG.11

Distribution of the radial mesh points.

Figure 11 shows the distribution of the radial mesh points. It must hold that

$$r_1 = -r_2$$

and

$$2a = r_{N+1} + r_N.$$

The other mesh points can be arbitrarily chosen. To approximate $\partial F/\partial r$, we require the auxiliary quantities

$$r_{J+1/2} = \frac{1}{2} (r_J + r_{J+1}),$$

$$d_J = r_J - r_{J-1},$$

and

$$d_{J+1} = r_{J+1} - r_J.$$

Formulation of difference equation

We approximate $\frac{\partial F}{\partial t}$ by $\frac{1}{\Delta T} \cdot [\hat{F}_J - F_J]$,

$$S \text{ by } \frac{1}{2} \cdot [\hat{S}_J + S_J],$$

$$\frac{\partial}{\partial r} \left[r \frac{\partial F}{\partial r} \right] \text{ by } \frac{1}{d_{J+1/2}} \left(\left[r \frac{\partial F}{\partial r} \right]_{r+1/2} - \left[r \frac{\partial F}{\partial r} \right]_{r+1/2} \right),$$

$$\left[r \frac{\partial F}{\partial r} \right]_{r+1/2} \text{ by } \frac{r_{J+1/2}}{2d_{J+1}} [\hat{F}_{J+1} - \hat{F}_J + F_{J+1} - F_J]$$

and $-\left[r \frac{\partial F}{\partial r} \right]_{r-1/2} \text{ by } \frac{r_{J-1/2}}{2d_J} [\hat{F}_{J-1} - \hat{F}_J + F_{J-1} - F_J].$

There is thus a similarity to, for example, the implicit scheme given by RICHTMYER /11/. Inserting these approximations in the partial differential equation yields

$$A_J \hat{F}_{J+1} + B_J \hat{F}_J + C_J \hat{F}_{J-1} = D_J$$

where $A_J = r_{J+1/2} / [d_{J+1} (\hat{s}_J + s_J) r_J d_{J+1/2}]$,

$$C_J = r_{J-1/2} / [d_J (\hat{s}_J + s_J) r_J d_{J+1/2}]$$
 ,

$$B_J = -A_J - C_J - R_T$$

$$R_T = 1/DT$$

and $D_J = A_J(F_J - F_{J+1}) + C_J(F_J - F_{J-1}) - R_T F_J$.

These equations are further rearranged to give the recursion formulae

$$\hat{F}_J = H_J \hat{F}_{J+1} + U_J$$

with $U_J = (D_J - U_{J-1} C_J) / (B_J + C_J H_{J-1})$

and $H_J = -A_J / (B_J + C_J H_{J-1})$.

From the boundary condition $F_1 = F_2$

it follows that $H_1 = 1$

and $U_1 = 0$.

This allows all U_J and H_J to be calculated in succession. From

the boundary condition $F(r = a) = G$

it follows that $\frac{1}{2} (\hat{F}_N + \hat{F}_{N+1}) = \hat{G}$

and $\hat{F}_{N+1} = \frac{2 \hat{G} - U_N}{1 + H_N}$.

This also allows the F_J to be calculated in succession. This algorithm was provided by **D. DUECHS**.

```

C GGELER'S PHASENBEZIEHUNG, SEGMENT G O E P A R
ISN 0002 REAL*4 IO , JZ(202) , LAMBDA , MO
ISN 0003 DIMENSION COSOMZ(637), S(57), NPR(77)
ISN 0004 COMMON /SIF/ EZ(57), R(57), RD(202), SIG(57), Z(17,77)
1 ,A,AL, BTOR,DR,DT, FR,OM,P,QF, RG,RSOND, SIGO, VERS, VC,VG, ZEIT
2 , MI(4), NI(4), LMA, NP, NT
COMMON /FUR/ DE(5), DL(5), RQ(5), SHEAR(5)
ISN 0005 READ 180, (MI(J),J=1,3) , (NI(J),J=1,3)
ISN 0006 PRINT 91
ISN 0007 READ 180, ( NPR(J), J=1,27)
ISN 0008 PRINT 180, ( NPR(J), J=1,27)
ISN 0009 10 READ 312, LMA, NP, NT, A,AL, BTOR, FR,P,RG, RSOND, SIGO, VC, VG
ISN 0010 L1 = LMA + 1
ISN 0011 MO = 1.25664E-6
ISN 0012 SIGO = SIGO * 1.E7
ISN 0013 OM = 6.2832 * FR
ISN 0014 UMFANG = 6.2832 * RG
ISN 0015 QF = 6.2832 * BTOR / (MO *RG)
ISN 0016 DR = AL / (LMA - 1.)
ISN 0017 DT = 6.2832 / ( OM* NT)
ISN 0018 VERS = (AL/A)**2
ISN 0019 EC = VC / UMFANG
ISN 0020 EG = VG / UMFANG
ISN 0021 RT = 1. / DT
ISN 0022 DD 2 L=1,L1
ISN 0023 R(L) = DR*( L - 1.5)
ISN 0024 RD(L) = R(L) / AL
ISN 0025 BASIS = 1.- VERS* RD(L)**2
ISN 0026 SIG(L) = 0.
ISN 0027 IF ( BASIS. LE. 1.E-6) GO TO 1
ISN 0028 SIG(L) = SIGO * BASIS**P
ISN 0029 1 S(L) = MO * SIG(L)
ISN 0030 2 EZ(L) = EG
ISN 0031 CALL FORM ( COSOMZ , NT )
ISN 0032 PRINT 92
ISN 0033 PRINT 110, (COSOMZ(J), J=1,NT)
ISN 0034 ZEIT = 0.
ISN 0035 EL = 0.
ISN 0036 LS = 1
ISN 0037 CALL SIGFRI ( JZ, Q, LS)
ISN 0038 DO 7 JP=1,NP
ISN 0039 DO 7 JT=1,NT
ISN 0040 ZEIT = ZEIT + DT
ISN 0041 ED = EG + EC* COSOMZ(JT)
ISN 0042 CALL PAPCYL ( EZ, S, DR, EL, ED, RT, LMA)
ISN 0043 J = JT + (JP-1)*NT
ISN 0044 IF (NPR(LS). NE. J) GO TO 7
ISN 0045 LS = LS + 1
ISN 0046 CALL SIGFRI ( JZ , Q , LS)
ISN 0047 7 EL = ED
ISN 0048 LAMBDA = 1./ ( AL* SQRT( MO *SIGO *FR * 6.2832))
ISN 0049 PRINT 98
ISN 0050 PRINT 95

```

```

ISN 0054      PRINT 313, LMA, NP, NT, A,AL, BTOR, FR,P,RG, RSOND, SIGO, VC, VG
ISN 0055      PRINT 101,  VERS , DT , LAMBDA
ISN 0056      PRINT 93
ISN 0057      PRINT 94,  (MI(J), NI(J), J=1,3) , (MI(J), NI(J), J=1,3)
1              , (MI(J), NI(J), J=1,3) , (MI(J), NI(J), J=1,3)
ISN 0058      DO 8      L=1,LS
ISN 0059      8 PRINT 107,      ( Z(K,L) , K=1,16)
ISN 0060      DM = 0.
ISN 0061      HM = 0.
ISN 0062      SM = 0.
ISN 0063      DO 9      L=8,LS
ISN 0064      SM = SM + (Z(14,L) + Z(14,L-1)) * (Z(1,L) - Z(1,L-1))
ISN 0065      DM = DM + (Z( 4,L) + Z( 4,L-1)) * (Z(1,L) - Z(1,L-1))
ISN 0066      9      HM = HM + (Z(15,L) + Z(15,L-1)) * (Z(1,L) - Z(1,L-1))
ISN 0067      HM = HM * 0.0795775
ISN 0068      DM = DM * 0.0795775
ISN 0069      SM = SM * 0.0795775
ISN 0070      PRINT 103,  DM, SM, HM
ISN 0071      CALL ZEICH ( Z , 7, LS)
ISN 0072      GO TO 10
ISN 0073      91 FORMAT(/10H      NPR)
ISN 0074      92 FORMAT(/10H      COSOMZ)
ISN 0075      93 FORMAT(/123H      D E L S      I N S E L BREITE
1      RADIUS DER Q-FLAECHE      D B / B      (X)      (KA)      (KW)      (GAU
2SS))
ISN 0076      94 FORMAT(/9H      OMT,I5,I1,I5,I1,I5,I1,I9,I1,I6,I1,I6,I1,I9,I1,I5,I
11,I5,I1,I9,I1,I5,I1,I5,I1,27H      IR      HEIZ      BTHETA)
ISN 0077      95 FORMAT(/102H      LMAX      NP      NT      A      AL      BTOR      FR
1      P      RG      RSOND      SIGO      VC      VG)
ISN 0078      98 FORMAT (1H1)
ISN 0079      101 FORMAT(/12H      VERS=,F7.2,12H      DT=,1PE9.2,12H      LAMBDA
1=,OPF7.4)
ISN 0080      103 FORMAT(/46H      VALUES AVERAGED OVER ONE PERIOD      DM=,F4.1,
147X, 2F8.1)
ISN 0081      107 FORMAT( F10.3 , 3F6.1 , F10.3, 2F7.3, F10.2, 2F6.2, F10.3, 2F7.3
1      , 4F8.2)
ISN 0082      110 FORMAT( 10F12.4)
ISN 0083      111 FORMAT( F12.3, 1P11E10.2)
ISN 0084      18C FORMAT( 1B14)
ISN 0085      312 FORMAT( 3I4 , 10F6.2)
ISN 0086      313 FORMAT( I10, 2I6, 7F8.2, 1PE9.2, 0P2F8.2)
ISN 0087      END

```

```

ISN 0002      SUBROUTINE SIGFRI ( JZ, Q, LS)
ISN 0003      REAL*4      IR , JZ(202), JZH
ISN 0004      DIMENSION  RF(202)
ISN 0005      COMMON /FUR/  DE(5) , DL(5) , RQ(5) , SHEAR(5)
ISN 0006      COMMON /SIF/  EZ(57), R(57), RD(202), SIG(57), Z(17,77)
1      ,A,AL, BTOR,DR,DT, FR,OM,P,QF, RG,RSOND, SIGO, VERS, VC,VG, ZEIT
2      , MI(4), NI(4), LMA, NP, NT

ISN 0007      JWRITE = 0
ISN 0008      OMT = OM * ZEIT
ISN 0009      IF (JWRITE. LE. 1)      GO TO 1
ISN 0011      PRINT 98
ISN 0012      PRINT 101,      LS, ZEIT, OMT
ISN 0013      PRINT 92
ISN 0014      PRINT 313,      LMA, NP, NT, A,AL, BTDR, FR,P,RG, RSOND, SIGO, VC, VG
ISN 0015      PRINT 94
ISN 0016      PRINT 111,      VERS
ISN 0017      PRINT 93
ISN 0018      1      SJ = 0.
ISN 0019      HEIZ = 0.
ISN 0020      DO 5      L=1,LMA
ISN 0021      RM = 0.5* ( R(L) + R(L+1))
ISN 0022      RF(L) = 0.5* ( RD(L) + RD(L+1))
ISN 0023      SIGM = 0.5* (SIG(L) + SIG(L+1))
ISN 0024      EZM = 0.5* ( EZ(L) + EZ(L+1))
ISN 0025      JZ(L) = SIGM * EZM
ISN 0026      SER = 0.
ISN 0027      IF (L. LE. 1)      GO TO 4
ISN 0029      SER = SIG(L) * EZ(L) * R(L)
ISN 0030      4      SJ = SJ + SER
ISN 0031      HEIZ = HEIZ + SER* EZ(L)
ISN 0032      IR = 6.2832 * DR * SJ
ISN 0033      Q = QF * RM**2 / ABS( IR + 1.E-7)
ISN 0034      IF ( JWRITE. LE. 1)      GO TO 5
ISN 0036      PRINT 111, RF(L), RM , EZ(L), JZ(L), IR, Q
ISN 0037      5 CONTINUE
ISN 0038      HEIZ = HEIZ * DR * 0.039478 * RG
ISN 0039      CALL FURTH( RF, JZ, LMA , Q, -1., 100, 0., MI, NI, 3)
ISN 0040      RSP = AL / RSOND
ISN 0041      FAKTOR = 1.25E+6 *RSOND *BTOR /(AL *RG *IR)
ISN 0042      DO 7      K=2,4
ISN 0043      K1 = K + 3
ISN 0044      K2 = K + 6
ISN 0045      K3 = K + 9
ISN 0046      M = MI(K-1)
ISN 0047      Z(K1,LS) = DL(K-1)
ISN 0048      Z(K2,LS) = RQ(K-1)
ISN 0049      Z(K3,LS) = SHEAR(K-1) * RQ(K-1) * DL(K-1)**2 * AL**2 * FAKTOR
1      * M * RSP**M * 100.
ISN 0050      7      Z(K,LS) = DE(K-1)
ISN 0051      Z(1,LS) = OMT
ISN 0052      Z(14,LS) = IR * 1.E-3
ISN 0053      Z(15,LS) = HEIZ
ISN 0054      Z(16,LS) = 2.E-3 * IR / RSOND

```

```

ISN 0055           Z(17,LS) = 3.14
ISN 0056           RETURN
ISN 0057           92 FORMAT(/102H          LMAX      NP      NT          A          AL      BTOR      FR
1                P          RG      RSOND      SIGO          VC          VG)
ISN 0058           93 FORMAT(/60H          RD          RM          EZ          JZ          IR
1                Q)
ISN 0059           94 FORMAT(/10H          VERS)
ISN 0060           98 FORMAT( 1H1)
ISN 0061           101 FORMAT(/9H          LS=,I2,10H          ZEIT=,1PE10.3,10H          OMT=,OPF7.3)
ISN 0062           111 FORMAT( F12.3, 1P11E10.2)
ISN 0063           313 FORMAT( I10, 2I6, 7F8.2, 1PE9.1, OP2F8.2)
ISN 0064           END

```

```

ISN 0002           SUBROUTINE PARCYL ( F, S, DR, G, GD, RT, N)
ISN 0003           DIMENSION F(57), FD(57), S(57), SD(57)
ISN 0004           1          , A(57), B(57), C(57), D(57), H(57), U(57)
ISN 0005           F(N+1) = 2.*G - F(N)
ISN 0006           DO 1      J=1,N
ISN 0007           DRS = DR**2 * (J - 1.5) * (S(J) + S(J))
ISN 0008           A(J) = (J - 1.) / DRS
ISN 0009           C(J) = (J - 2.) / DRS
ISN 0010           B(J) = - A(J) - C(J) - RT
ISN 0011           FM = F(1)
ISN 0012           IF ( J. LE. 2)      GO TO 1
ISN 0013           FM = F(J-1)
ISN 0014           1          D(J) = A(J)*( F(J) -F(J+1)) + C(J)*( F(J) -FM) - F(J)*RT
ISN 0015           H(1) = 1.
ISN 0016           U(1) = 0.
ISN 0017           DO 2      J=2,N
ISN 0018           BCH = B(J) + C(J) *H(J-1)
ISN 0019           U(J) = (D(J) - C(J)*U(J-1)) / BCH
ISN 0020           2          H(J) = - A(J) / BCH
ISN 0021           FD(N+1) = (2.*GD - U(N)) / (1.+ H(N))
ISN 0022           DO 3      J=1,N
ISN 0023           K = N + 1 - J
ISN 0024           3          FD(K) = H(K) *FD(K+1) + U(K)
ISN 0025           DO 5      J=1,N
ISN 0026           5          F(J) = FD(J)
ISN 0027           RETURN
ISN 0028           END

```


ISN 0002

```

SUBROUTINE FURTH(RI,AJ,NPIN,QB,BW,NP,JOTAO,MI,NI,NMN)
C TEARING MODE STABILITY IN STRAIGHT CYLINDER
C FOLLOWING GLASSER,FURTH,RUTHERFORD
C STORED IN KAL:FURTH.FURTH; FILE SHARED BY ALL AMOS USERS
C-----
C MEANING OF INPUT PARAMETERS
C-----
C RADIAL COORDINATE NORMALIZED BY PLASMA RADIUS A
C RI ..... RADIAL COORDINATE OF POINTS IN WHICH PLASMA
C CURRENT DENSITY IS GIVEN
C AJ ..... VALUES OF CURRENT DENSITY IN POINTS RI (IN ARBI-
C TRARY UNITS
C NPIN ..... NUMBER OF POINTS OF RI,AJ
C ***** R(1) MUST BE 0.,R(NPIN) MUST BE 1.*****
C QB ..... Q OF PLASMA CURRENTS AT PLASMA BOUNDARY
C BW ..... RADIUS OF CONDUCTING WALL (SPECIFY A NEGAT. VAL-
C UE IF NO CONDUCTING WALL PRESENT)
C NP ..... NR OF GRID POINTS USED FOR COMPUTING MARGINAL
C MHD MODE IN BOTH INTERVAL (0,R SINGULAR) AND IN
C (R SINGULAR,1)
C JOTAO ..... JOTA OF EXTERNAL WINDINGS
C MI,NI ..... VECTORS OF THE (M,N) VALUES FOR THE MODES TO BE
C EXAMINED
C NMN ..... NUMBER OF (M,N) PAIRS TO BE EXAMINED
C-----

```

ISN 0003

```

REAL*4 RI(202),AJ(202),AJ2(202),DU1(202),DU2(202),Q(202),Q2(202),
X AI(808),R(202),Y(202),YSING(202),YTOT(202),
X RL(202),RP(202),YDL(202),YDR(202)

```

ISN 0004

REAL*4 JOTAO

ISN 0005

DIMENSION XP(21),YP(21),XZ(2),YZ(2),XX(2),YX(2),TEXT(5)

ISN 0006

COMMON /FUR/ DE(5),BR(5),RQ(5),SHEAR(5)

ISN 0007

INTEGER*4 MI(4),NI(4),IOUTP(4)

ISN 0008

DATA ERROR/1.E-05/

ISN 0009

```

RHS(RD) = -( ( AKS - G * (RD-RS) ) / (RD-RS)
X + ALL * (AKS * (AKSP + A2MP1/RD - G * (RD-RS) ) )
X + (RD-RS) * ALL * (AKS * AKSP * (A2MP1/RD - .5 * G * (RD-RS) ) )
X + 1.5 * AKS * AKSP + A2MP1/RD * AKS
X + .5 * (RD-RS) * A2MP1/RD * AKS * AKSP

```

```

C-----
C SPLINING OF CURRENT PROFILE
C-----

```

ISN 0010

DO 1 K=1,5

ISN 0011

DE(K) = 0.

ISN 0012

BR(K) = 0.

ISN 0013

RQ(K) = 0.

ISN 0014

1 SHEAR(K) = 0.

ISN 0015

AJ2(1) = 0.

ISN 0016

D2 = RI(NPIN) - RI(NPIN-2)

ISN 0017

D1 = RI(NPIN) - RI(NPIN-1)

ISN 0018

```

AJ2(NPIN) = (AJ(NPIN-2)*D1**2 - AJ(NPIN-1)*D2**2
X + AJ(NPIN)*(D2**2 - D1**2) )

```

```

X          / (D2**2*D1-D1**2*D2)
ISN 0019  CALL CUBIC3(NPIN,RI,AJ,AJ2,DU1,DU2)
C-----
C  COMPUTATION OF Q -PROFILE AND RESCALING OF J
C-----
ISN 0020  Q(1) = 0.
ISN 0021  DO 111 I = 2,NPIN
ISN 0022  DX = RI(I) -RI(I-1)
ISN 0023  A = (AJ2(I)-AJ2(I-1))/(6.*DX)
ISN 0024  B = .5*AJ2(I-1)
ISN 0025  C = (AJ(I)-AJ(I-1))/DX - DX/6. * (AJ2(I) + 2.*AJ2(I-1))
ISN 0026  D = AJ(I-1)
ISN 0027  Q(I) = Q(I-1)
X + (((0.2*A*DX + 0.25*(A*RI(I-1)+B))*DX
X      + (B*RI(I-1)+C)/3.)*DX
X      + 0.5 *(C*RI(I-1)+D))*DX
X      + D*RI(I-1))*DX
ISN 0028  111 CONTINUE
ISN 0029  COEF = 1./(6.2831853*Q(NPIN))
ISN 0030  DO 112 I = 1,NPIN
ISN 0031  AJ(I) = AJ(I)*COEF
ISN 0032  112 AJ2(I) = AJ2(I)*COEF
ISN 0033  Q(1) = QB/(3.1415926*AJ(1))
ISN 0034  Q(1) = Q(1) / (1.+Q(1)*JOTAO)
C-----
C-----
ISN 0035  COEF = QB*Q(NPIN)
ISN 0036  DO 113 I = 2,NPIN
ISN 0037  Q(I) = COEF*RI(I)**2/Q(I)
ISN 0038  Q(I) = Q(I)/(1.+Q(I)*JOTAO)
ISN 0039  113 CONTINUE
ISN 0040  Q2(1) = 0.
ISN 0041  Q2(NPIN) = 2.*QB
ISN 0042  QBB = QB/(1.+ QB*JOTAO)
ISN 0043  CALL CUBIC3(NPIN,RI,Q,Q2,DU1,DU2)
C-----
C  CHOICE OF M,N - MODE AND LOCATION OF RESONANT SURFACE
C-----
ISN 0044  IMN = 0
C-----
ISN 0045  201 IMN = IMN + 1
C-----
ISN 0046  IF (IMN.GT.NMN)RETURN
ISN 0048  M = MI(IMN)
ISN 0049  N = NI(IMN)
ISN 0050  DLL=0.
ISN 0051  IF (BW.LT.0.) GO TO 221
ISN 0053  GAM = M*(1.+BW***(2*M))/(1.-BW***(2*M))
ISN 0054  GO TO 222
ISN 0055  221 GAM = -M
ISN 0056  222 CCNTINUE
ISN 0057  A2MPI = 2*M+1
ISN 0058  QRES = FLOAT(M) / FLOAT(N)
ISN 0059  IF (M.LT.N*Q(1)) GO TO 201
ISN 0061  IF (M.GT. N*QBB) GO TO 500
ISN 0063  RRES = (QRES-Q(1))/(Q(NPIN) - Q(1))
C-----
ISN 0064  202 CALL ODINT (RI,Q,Q2,NPIN,RRES,QR,QDR,IFLAG)

```

```

ISN 0065      RNEW = PRES + (QRES-QR)/QDR
ISN 0066      IF (RNEW.GT.1.) RNEW = .5*(1.+RRES)
ISN 0068      IF (RNEW.LT.0.) RNEW = .5*RRES
ISN 0070      DEL = RNEW - RRES
ISN 0071      RRES = RNEW
ISN 0072      IF (ABS(DEL).GT.ERROR) GO TO 202

```

```

C-----
C  SOLUTION FOR THE REGION R < RS
C-----

```

```

ISN 0074      602  RS = RRES
ISN 0075      DR = RS/(NP+.5)
ISN 0076      R(1) = .5*DR
ISN 0077      DO 211 I = 2, NP
ISN 0078      211  R(I) = R(I-1) + DR
ISN 0079      CALL CDINT (R1, AJ, AJ2, NPIN, RS, AR, ADR, IFLAG)
ISN 0080      CALL CDINT (R1, Q, Q2, NPIN, RS, QR, QDR, IFLAG)
ISN 0081      SHEA = QDR / QR**2
ISN 0082      AKS = -6.2831853 * QR*ADR / (QB*RS*N*QDR) *M
ISN 0083      AKSP = AKS - A2MP1/RS
ISN 0084      R(NP+1) = RS

```

```

C-----
C  SET-UP OF COEFFICIENT MATRIX ACCORDING TO 18 OCT/4 - 1976
C-----

```

```

ISN 0085      DL = 2. *R(1)
ISN 0086      CALL CDINT (R1, AJ, AJ2, NPIN, R(1), AR, ADR, IFLAG)
ISN 0087      CALL CDINT (R1, Q, Q2, NPIN, R(1), QR, QDR, IFLAG)
ISN 0088      G = 6.2831853 * QR*ADR / (R(1)*QB*(M-N*QR)) *M
ISN 0089      ALL = ALOG (RS-R(1))
ISN 0090      A1(2) = -1. -A2MP1 - G*DL**2
ISN 0091      A1(3) = 1. + A2MP1
ISN 0092      A1(4) = DL**2*RHS(R(1)) - DL*(1.-A2MP1)*AKS*(ALOG(RS) + 1.
X             -AKSP * RS * (ALOG(RS) + .5))
ISN 0093      DO 301 I = 2, NP
ISN 0094      NO = 4*(I-1)
ISN 0095      DR = R(I+1)-R(I)
ISN 0096      DL = R(I) - R(I-1)
ISN 0097      CALL CDINT (R1, AJ, AJ2, NPIN, R(I), AR, ADR, IFLAG)
ISN 0098      CALL CDINT (R1, Q, Q2, NPIN, R(I), QR, QDR, IFLAG)
ISN 0099      G = 6.2831853 * QR*ADR / (R(I)*QB*(M-N*QR))*M
ISN 0100      ALL = ALOG(RS-R(I))
ISN 0101      A1(NO+1) = (2. - A2MP1/R(I)*DR)*DR
ISN 0102      A1(NO+2) = (-2. + A2MP1/R(I)*(DR-DL) - G*DR*DL)*(DR+DL)
ISN 0103      A1(NO+3) = (2. + A2MP1/R(I)*DL)*DL
ISN 0104      A1(NO+4) = DR*DL*(DR+DL)*RHS(R(I))
ISN 0105      301  CONTINUE
ISN 0106      CALL LGLSS(A1, Y, NP-1, 0., 6)
ISN 0107      DO 302 I = 1, NP
ISN 0108      ALL = ALOG(RS-R(I))
ISN 0109      YSING(I) = 1.+AKS*(R(I)-RS)*ALL
X             + .5*AKS*AKSP *(R(I)-RS)**2*ALL
ISN 0110      YTOT(I) = (R(I)/RS)**M *(Y(I) + YSING(I))
ISN 0111      302  CONTINUE
ISN 0112      311  YS1 = (Y(NP-1) - 4.*Y(NP))/(2.*(R(NP) - R(NP-1)))

```

```

C-----
ISN 0113      NPPI = NP+1
ISN 0114      DELL = DR
ISN 0115      DO 321 I = 1, NP
ISN 0116      RL(I) = R(I)

```

```

ISN 0117      321  Y(I) = YTOT(I)
ISN 0118      RL(NP+1) = RS
ISN 0119      Y(NP+1) = 1.
ISN 0120      CALL DET3(DR,Y,YDL,NPPI,IER)
C             STATEMENTS TO ADD IF DPSI/DR / PSI USED
C             DO 325 I = 1,NPPI
C 325         YDL(I) = YDL(I)/Y(I)
-----
ISN 0121      YDI = 0.
ISN 0122      YDD = 1.
-----
C             SOLUTION FOR REGION R > RS
-----
ISN 0123      NR = NP + 1
ISN 0124      DR = (1.-RS)/(NR-.5)
ISN 0125      NRP1 = NR + 1
ISN 0126      R(1) = RS
ISN 0127      DO 401 I = 2,NRP1
ISN 0128      401  R(I) = R(I-1) + DR
ISN 0129      DO 402 I = 2,NR
ISN 0130      NO = 4*(I-2)
ISN 0131      DR = R(I+1)-R(I)
ISN 0132      DL = R(I) - R(I-1)
ISN 0133      CALL DDINT (R1,AJ,AJ2,NPIN,R(I),AR,ADR,I FLAG)
ISN 0134      CALL DDINT (R1,Q ,Q2 ,NPIN,R(I),QR,QDR,I FLAG)
ISN 0135      G = 6.2831853 * QR*ADR/ (R(I)*QB*(M-N*QR))*M
ISN 0136      ALL = ALOG(R(I)-RS)
ISN 0137      A1(NO+1) = (2. - A2MP1/R(I)*DR)*DR
ISN 0138      A1(NO+2) = (-2. + A2MP1/R(I)*(DR-DL) - G*DR*DL)*(DR+DL)
ISN 0139      A1(NO+3) = (2. + A2MP1/R(I)*DL)*DL
ISN 0140      A1(NO+4) = DR*DL*(DR+DL)*RHS(R(I))
ISN 0141      402  CONTINUE
ISN 0142      A1(1) = 0.
ISN 0143      NO = 4*(NR-1)
ISN 0144      A1(NO+1) = -(1.+5*DR*(GAM-M))
ISN 0145      A1(NO+2) = 1.-5*DR*(GAM-M)
ISN 0146      A1(NO+3) = 0.
ISN 0147      ALL = ALOG (1.-RS)
ISN 0148      A1(NO+4) = -DR*(AKS*(ALL+1.)+AKS*AKSP*(1.-RS)*(ALL+.5)
X - (GAM-M)*(1.+AKS*(1.-RS)*ALL + .5*AKS*AKSP*(1.-RS)**2*ALL))
ISN 0149      CALL LGLSS(A1,Y,HR-1,0.,6)
ISN 0150      DO 404 I = 2,NR
ISN 0151      J = I - 1
ISN 0152      ALL = ALOG(R(I)-RS)
ISN 0153      YSING(J) = 1.+AKS*(R(I)-RS)*ALL
X + .5*AKS*AKSP *(R(I)-RS)**2*ALL
ISN 0154      YTOT(J) = (R(I)/RS)**M *(Y(J) + YSING(J))
ISN 0155      404  CONTINUE
ISN 0156      411  YS2 = (4.*Y(1) - Y(2))/(2.*(R(2)-R(1)))
ISN 0157      N9 = NR - 1
ISN 0158      SHEAR(IMN) = YTOT(N9) * SHEA
-----
ISN 0159      RR(1) = RS
ISN 0160      YSING(1) = 1.
ISN 0161      DELR = DR
ISN 0162      DO 421 I = 2,NPPI
ISN 0163      RR(I) = R(I)
ISN 0164      421  YSING(I) = YTOT(I-1)

```

```

ISN 0165      CALL DET3(DR,YSING,YDR,NPPI,IER)
C             STATEMENTS TO ADD IF DPSI/DR / PSI USED
C             DO 425 I = 1,NPPI
C 425         YDR(I) = YDR(I)/YSING(I)
C-----
ISN 0166      DELS = YS2 - YS1
C-----
ISN 0167      IF(DELS .LT.0.) GO TO 210
ISN 0169      DEL = DELL
ISN 0170      IF(DELR.LT.DELL) DEL = DELR
ISN 0172      DLL = DEL
ISN 0173      REL = RS-DLL
ISN 0174      RER = RS+DLL
ISN 0175      CALL ALI(REL,RL,YDL,YDEL,NPPI,IER)
ISN 0176      CALL ALI(RER,RR,YDR,YDER,NPPI,IER)
ISN 0177      DELSL = YDER - YDEL
ISN 0178      IF(DELSL.GT.0) GO TO 461
ISN 0180      GO TO 210
ISN 0181      461 CONTINUE
ISN 0182      DLL = DLL + DEL
ISN 0183      REL = RS-DLL
ISN 0184      RER = RS+DLL
ISN 0185      CALL ALI(REL,RL,YDL,YDEL,NPPI,IER)
ISN 0186      CALL ALI(RER,RR,YDR,YDER,NPPI,IER)
ISN 0187      DELSL = YDER - YDEL
C             X             + M*AKS/P.S
C             X*((RS+DLL)/RS)**(M-1)*(DLL*ALOG(DLL)+0.5*AKSP*DLL**2*ALOG(DLL))
C             X + ((RS-DLL)/RS)**(M-1)*(DLL*ALOG(DLL)-0.5*AKSP*DLL**2*ALOG(DLL))
C             X             + AKS
C             X*((RS+DLL)/RS)**M *(ALOG(DLL)+1.+0.5*AKSP*(2.*DLL*ALOG(DLL)+DLL))
C             X-((RS-DLL)/RS)**M *(ALOG(DLL)+1.-0.5*AKSP*(2.*DLL*ALOG(DLL)+DLL))
ISN 0188      IF(ABS(DELSL).GE.(100.*ERROR*DELS )) GO TO 472
ISN 0190      462 CONTINUE
ISN 0191      GO TO 210
ISN 0192      472 IF (DELSL) 473,462,474
ISN 0193      473 DLL = DLL - DEL
ISN 0194      DEL = 0.5*DEL
ISN 0195      GO TO 461
ISN 0196      474 IF((REL.GT.RL(2)).AND.(RER.LT.RR(NP-1))) GO TO 461
C-----
ISN 0198      GO TO 210
C-----
C-----
C             SOLUTION IF Q RES IN VACUUM
C-----
ISN 0199      500 NR = NP
ISN 0200      IF (JOTAO*QRES.GE.1.) GO TO 505
ISN 0202      RS = SQRT(QRES/QB/(1.-JOTAO*QRES))
ISN 0203      IF ((BW.GT.0.) .AND. (RS.GT.BW)) GO TO 201
ISN 0205      GAM = 2.*M*RS**(2*M)/(1.-RS**(2*M))
ISN 0206      DR = 1./NR
ISN 0207      R(1) = .5*DR
ISN 0208      NRP1 = NP+1
ISN 0209      DO 501 I = 2,NRP1
ISN 0210      501 R(I) = P(I-1) +DR
ISN 0211      CALL ODINT (RI,AJ,AJ2,NPIN,R(1),AR,ADR,IFLAG)
ISN 0212      CALL CDINT (RI,Q ,Q2 ,NPIN,R(1),QR,QDR,IFLAG)
ISN 0213      G = 6.2831853 * QR*ADR*M/ (R(1)*QB*(M-N*CR))

```

ISN 0002

```

-----
C      SUBROUTINE LGLSS(A,X,N,EPS,NOUT)
-----
C      LOESUNG EINES LINEAREN GLS A*X=D ,A:TRIDIAGONALMATRIX
C      AUF A WERDEN DIE KOEFFIZIENTEN JEDER GLEICHUNG
C      A(I)*X(I-1)+B(I)*X(I)+C(I)*X(I+1)=D(I)
C      F-INTEREINANDER GESPEICHERT.
C      DIE SPEICHERBFLEGUNG SIEHT ALSO SO AUS:
C      1. ZEILE VON A: *,A(1),A(2),.....A(N)
C      2.  " " "  A* B(0),B(1),B(2),.....B(N)
C      3.  " " "  A: C(0),C(1),C(2),...C(N-1), *
C      4.  " " "  A: D(0),D(1),D(2),.....D(N)
C      A WIRD ZERSTOERT
C      X ENTHAELT DIE BERECHNETE LOESUNG
C      EPS: 0-SCHRANKE
C      NOUT: ALSGABEKANAL
C      BEMERKUNG:
C              DAS DURCHGEFUEHRTE VERFAHREN IST IN RICHTMYER MORTON :
C              '' DIFFERENCE METHODS FOR INITIAL VALUE PROBLEMS''
C              SEITE 199 FF BESCHRIEBEN
C              DIE OBIGEN BEZEICHNUNGEN ENTSPRECHEN IN RICHTMYER MORTON:
C
C              A(J)          :          -C(J)
C              DL = 2.*R(1)  :          R(1)
C              A1(2) = -1.-A2MP1 - G*DL**2
C              A1(3) = 1.+A2MP1
C              A1(4) = 0.
C              DO 502 I = 2,NP
C              NO = 4*(I-1)
C              DR = R(I+1)-R(I)
C              DL = R(I) - R(I-1)
C              CALL ODINT (RI,AJ,AJ2,NPIN,R(I),AR,ADR,I FLAG)
C              CALL CDINT (RI,Q ,Q2 ,NPIN,R(I),QR,QDR,I FLAG)
C              G = 6.2831853 * QR*ADR*M/(R(I)*QB*(M-N*QR))
C              A1(NO+1) = (2. - A2MP1/R(I)*DR)*DR
C              A1(NO+2) = (-2. + A2MP1/R(I)*(DR-DL) - G*DR*DL)*(DR+DL)
C              A1(NO+3) = (2. + A2MP1/R(I)*DL)*DL
C              502 A1(NO+4) = 0.
C              NO = 4* NP
C              A1(NO+1) = -(1.+5*DR*GAM)
C              A1(NO+2) = 1.-5*DR*GAM
C              A1(NO+3) = 0.
C              A1(NO+4) = -DR*GAM/RS**M
C              CALL LGLSS(A1,Y,NP,0.,6)
C              DO 504 I = 1,NR
C              YSING(I) = 0.
C              YTOT(I) = R(I)**M*Y(I)
C              504 CONTINUE
C              511 DD = (RS/BW) ** (2*M)
C              IF (BW.LT.0.) DD = 0.
C              DT = RS** (2*M)
C              DELS = M/RS = ((DD+1)/(DD-1) - ((Y(NR) + Y(NR+1))*RS**M - 2.*DT)
C              X / (1.-DT) + 1.)
C              505 CONTINUE
C              210 CONTINUE
C
C              DE(IMN) = DELS
C              BR(IMN) = DLL
C              RQ(IMN) = RS
C              81 FORMAT(/40H          IMN          DELS          DLL          RS)
C              82 FORMAT( I10, 5F10.3)
C              GO TO 201
C              END

```

```

ISN 0002          SUBROUTINE ODINT(X,F,FDD,NP,XP,FP,FDP,IFLAG)
ISN 0003          DIMENSION X(1),F(1),FDD(1)
C -----
C   GIVEN A FUNCTION F AND ITS SECOND DERIVATIVE FDD IN
C   NP POINTS X, COMPUTES THE FUNCTION AND ITS FIRST
C   DERIVATIVE IN XP
C -----
ISN 0004          IFLAG = 2
ISN 0005          IF((XP.LT.X(1)).OR.(XP.GT.X(NP))) RETURN
ISN 0007          IFLAG = 1
ISN 0008          DO 101 I = 2,NP
ISN 0009          IF (XP.GT.X(I)) GO TO 101
ISN 0011          DX = X(I) - X(I-1)
ISN 0012          A = (FDD(I) - FDD(I-1)) / (6.*DX)
ISN 0013          B = 0.5 *FDD(I-1)
ISN 0014          C = (F(I)-F(I-1))/DX - DX/6.*(FDD(I) + 2.*FDD(I-1))
ISN 0015          D = F(I-1)
ISN 0016          XX = XP -X(I-1)
ISN 0017          FP = ((A*XX+B)*XX+C)*XX + D
ISN 0018          FDP = (3.*A*XX + 2.*B)*XX + C
ISN 0019          RETURN
ISN 0020          101 CONTINUE
ISN 0021          RETURN
ISN 0022          END

```

```

ISN 0002          SUBROUTINE CUBIC3(N,X,Y,Y2,F,G)
C   KUBISCHER SPLINE MIT Y' AM RANDNVORGEHEN
C   H. SPAETH,PG. 46
C   DIMENSION X(1),Y(1),Y2(1),F(1),G(1)
ISN 0003          N1 = N-1
ISN 0004          J1 = 1
ISN 0005          H1 = C.
ISN 0006          R1 = Y2(1)
ISN 0007          G(1) = 0.
ISN 0008          F(1) = 0.
ISN 0009          DO 3 K=1,N
ISN 0010          IF (K. LE. N1) GO TO 1
ISN 0011          H2 = 0.
ISN 0012          R2 = Y2(N)
ISN 0013          GO TO 2
ISN 0014          1 J2 = K+1
ISN 0015          H2 = X(J2) - X(K)
ISN 0016          R2 = (Y(J2) - Y(K))/H2
ISN 0017          2 Z = 1./(2.*(H1+H2) - H1*G(J1))
ISN 0018          G(K) = Z*H2
ISN 0019          F(K) = Z*(6.*(R2-R1)-H1*F(J1))
ISN 0020          J1 = K
ISN 0021          H1 = H2
ISN 0022          R1 = R2
ISN 0023          3 CONTINUE
ISN 0024          Y2(N) = F(N)
ISN 0025          DO 4 J1 =1,N1
ISN 0026          K = N - J1
ISN 0027          Y2(K) = F(K) - G(K)*Y2(K+1)
ISN 0028          4 CONTINUE
ISN 0029          RETURN
ISN 0030          END

```

```

ISN 0002          SUBROUTINE DET3(H,Y,Z,NDIM,IER)
C
C
ISN 0003          DIMENSION Y(1),Z(1)
C
C          TEST OF DIMENSION
ISN 0004          IF(NDIM-3)4,1,1
C
C          TEST OF STEP SIZE
ISN 0005          1 IF(H)2,5,2
C
C          PREPARE DIFFERENTIATION LOOP
ISN 0006          2 HH=.5/H
ISN CC07          YY=Y(NDIM-2)
ISN 0008          B=Y(2)+Y(2)
ISN CC09          B=HH*(B+B-Y(3)-Y(1)-Y(1)-Y(1))
C
C          START DIFFERENTIATION LOOP
ISN CC10          DO 3 I=3,NDIM
ISN 0011          A=B
ISN CC12          B=HH*(Y(I)-Y(I-2))
ISN CC13          3 Z(I-2)=A
C
C          END OF DIFFERENTIATION LOOP
C
C          NORMAL EXIT
ISN 0014          IER=0
ISN CC15          A=Y(NDIM-1)+Y(NDIM-1)
ISN 0016          Z(NDIM)=HH*(Y(NDIM)+Y(NDIM)+Y(NDIM)-A-A+YY)
ISN 0017          Z(NDIM-1)=B
ISN CC18          RETURN
C
C          ERROR EXIT IN CASE NDIM IS LESS THAN 3
ISN CC19          4 IER=-1
ISN CC20          RETURN
C
C          ERROR EXIT IN CASE OF ZERO STEPSIZE
ISN 0021          5 IER=1
ISN 0022          RETURN
ISN 0023          END

ISN CC02          SUBROUTINE ALI (X,XARR,YARR,Y,NP,IER)
ISN 0003          DIMENSION XARR(1),YARR(1)
ISN 0004          IER = 1
ISN 0005          IF ((X.LT.XARR(1)).OR.(X.GT.XARR(NP))) GO TO 201
ISN CC07          DO 101 I = 2,NP
ISN CC08          IF (XARR(I).LT.X) GO TO 101
ISN 0010          Y = YARR(I-1) + (YARR(I) - YARR(I-1)) * (X - XARR(I-1)) /
X                (XARR(I) - XARR(I-1))
ISN 0011          GO TO 111
ISN 0012          101 CONTINUE
ISN 0013          111 RETURN
ISN 0014          201 IER = -1
ISN 0015          Y = -1.E65
ISN CC16          RETURN
ISN 0017          END

```



```

ISN CC02      SUBROUTINE ZEICH ( Z , L1 , L2 )
ISN C003      DIMENSION  X(77), Y(77), Y1(77), Y2(77), Y3(77), Y4(77), Z(17,77)
ISN C004      XMI = Z(1,L1)
ISN 0005      XMA = XMI + 4.8*( Z(1,L2) - Z(1,L1))
ISN 0006      YMI = - 10.
ISN 0007      YMA = + 80.
ISN C008      X(1) = XMI
ISN C009      Y(1) = YMI
ISN 0010      X(2) = XMI
ISN 0011      Y(2) = 20.
ISN 0012      X(3) = Z(1,L2)
ISN 0013      Y(3) = 20.
ISN 0014      X(4) = Z(1,L2)
ISN 0015      Y(4) = YMI
ISN 0016      X(5) = XMI
ISN C017      Y(5) = YMI
ISN 0018      CALL FRAME ( XMI , YMI , XMA , YMA )
ISN C019      CALL PLOTL ( X, Y, 5)
ISN C020      X(1) = XMI
ISN 0021      X(2) = Z(1,L2)
ISN 0022      Y(1) = 0.
ISN 0023      Y(2) = 0.
ISN 0024      CALL PLOTL ( X, Y, 2)
ISN C025      JMA = L2 - L1 + 1
ISN 0026      DO 1      J=1,JMA
ISN 0027          L = J - 1 + L1
ISN 0028          X(J) = Z(1,L)
ISN 0029          Y1(J) = Z(2,L)
ISN C030          Y2(J) = Z(3,L)
ISN 0031          Y3(J) = Z(4,L)
ISN 0032      1      Y4(J) = Z(5,L)
ISN C033      CALL FLOTLS( X, Y1, JMA)
ISN 0034      CALL PLOTLS( X, Y2, JMA)
ISN 0035      CALL FLOTL ( X, Y3, JMA)
ISN 0036          YMI = 0.
ISN 0037          YMA = 3.
ISN 0038          X(1) = XMI
ISN 0039          Y(1) = YMI
ISN C040          X(2) = XMI
ISN 0041          Y(2) = 1.
ISN 0042          X(3) = Z(1,L2)
ISN 0043          Y(3) = 1.
ISN 0044          X(4) = Z(1,L2)
ISN 0045          Y(4) = YMI
ISN C046          X(5) = XMI
ISN 0047          Y(5) = YMI
ISN C048      CALL FRAME ( XMI , YMI , XMA , YMA )
ISN C049      CALL PLOTL ( X, Y, 5)
ISN 0050      DO 3      K=8,11
ISN 0051      DO 2      J=1,JMA
ISN 0052          L = J - 1 + L1
ISN 0053          X(J) = Z(1,L)
ISN 0054          Y1(J) = Z(K,L)
ISN 0055          Y2(J) = Z(K,L) - Z(K-3,L)
ISN 0056      2      Y3(J) = Z(K,L) + Z(K-3,L)
ISN C057      CALL PLDTL ( X, Y1, JMA)
ISN 0058      CALL PLOTLS( X, Y2, JMA)
ISN C059      CALL PLOTLS( X, Y3, JMA)
ISN C060      3 CONTINUE
ISN 0061      RETURN
ISN C062      END

```

LHAX	NP	NT	A	AL	BTOR	FR	P	RG	RSOND	SIGC	VC	VG	(KA)	(KW)	(GAJSS)
41	7	100	0.13	0.11	2.80	400.00	5.76	0.70	0.16	1.40E+07	4.50	2.20			
VERS= 0.72 DT= 2.50E-05 LAMBCA= 0.0432															
D E L S I N S E L B R E I T E R A D I U S D E R Q - F L A E C H E D B / B (%)															
CMT	31	32	21	31	32	21	31	32	21	31	32	21	31	32	21
0.0	-4.4	-1.2	4.8	0.0	0.0	0.092	0.82	0.50	0.64	0.0	0.0	0.271	55.00	121.00	87.54
6.283	-5.7	2.7	6.3	0.0	0.014	0.112	0.80	0.52	0.64	0.0	0.002	0.540	52.54	113.13	656.80
12.566	-5.8	1.9	5.9	0.0	0.010	0.109	0.80	0.52	0.63	0.0	0.001	0.509	52.03	111.27	650.37
18.848	-5.8	1.7	5.9	0.0	0.010	0.107	0.80	0.51	0.63	0.0	0.001	0.491	51.74	110.12	646.72
25.131	-5.8	1.7	5.9	0.0	0.010	0.106	0.79	0.51	0.63	0.0	0.001	0.484	51.53	109.26	644.12
31.413	-5.8	1.7	6.0	0.0	0.009	0.106	0.79	0.51	0.63	0.0	0.001	0.479	51.36	108.56	642.05
37.655	-5.8	1.7	6.1	0.0	0.009	0.106	0.79	0.51	0.63	0.0	0.001	0.477	51.23	107.97	640.31
38.010	-5.9	1.3	4.9	0.0	0.007	0.102	0.80	0.51	0.63	0.0	0.001	0.410	52.14	110.54	651.79
38.324	-5.8	0.8	3.6	0.0	0.005	0.096	0.80	0.50	0.63	0.0	0.000	0.327	53.43	115.84	667.92
38.638	-5.3	0.1	2.3	0.0	0.005	0.085	0.82	0.50	0.63	0.0	0.000	0.228	54.97	123.46	687.11
38.952	-4.6	-0.7	1.1	0.0	0.0	0.061	0.83	0.50	0.63	0.0	0.0	0.106	56.60	132.41	707.48
39.266	-3.9	-1.7	0.2	0.0	0.0	0.016	0.84	0.50	0.64	0.0	0.0	0.007	58.16	141.32	727.02
39.580	-3.4	-2.6	-0.1	0.0	0.0	0.0	0.85	0.50	0.65	0.0	0.0	0.0	59.51	148.76	743.82
39.854	-3.1	-3.6	0.5	0.0	0.0	0.018	0.86	0.50	0.66	0.0	0.0	0.008	60.50	153.57	756.21
40.208	-3.1	-4.4	1.8	0.0	0.0	0.040	0.87	0.51	0.67	0.0	0.0	0.040	61.04	155.18	763.00
40.523	-3.2	-4.5	3.4	0.0	0.0	0.061	0.87	0.51	0.67	0.0	0.0	0.097	61.08	153.64	763.49
40.837	-3.4	-5.0	5.0	0.0	0.0	0.076	0.86	0.51	0.67	0.0	0.0	0.168	60.61	149.61	757.63
41.151	-3.6	-4.5	6.3	0.0	0.0	0.087	0.86	0.52	0.68	0.0	0.0	0.242	59.68	144.03	745.00
41.465	-3.8	-3.5	7.3	0.0	0.0	0.095	0.85	0.52	0.67	0.0	0.0	0.319	58.38	137.87	729.72
41.775	-4.0	-2.3	8.0	0.0	0.0	0.101	0.84	0.53	0.67	0.0	0.0	0.390	56.83	131.84	710.37
42.093	-4.2	-1.0	8.4	0.0	0.0	0.105	0.83	0.53	0.66	0.0	0.0	0.455	55.19	126.29	689.86
42.407	-4.3	0.2	8.6	0.0	0.005	0.108	0.82	0.52	0.66	0.0	0.000	0.508	53.61	121.29	670.17
42.721	-4.6	1.0	8.6	0.0	0.005	0.109	0.81	0.52	0.65	0.0	0.000	0.543	52.26	116.75	653.22
43.036	-4.8	1.6	8.3	0.0	0.009	0.110	0.80	0.52	0.64	0.0	0.001	0.558	51.25	112.70	633.47
43.350	-5.1	1.9	7.8	0.0	0.010	0.109	0.79	0.52	0.64	0.0	0.001	0.553	50.70	109.41	611.73
43.664	-5.5	2.0	7.1	0.0	0.010	0.108	0.79	0.51	0.63	0.0	0.001	0.524	50.65	107.43	633.11
43.915	-5.7	1.8	6.4	0.0	0.010	0.107	0.79	0.51	0.63	0.0	0.001	0.487	50.98	107.26	637.19
43.978	-5.8	1.8	6.2	0.0	0.009	0.106	0.79	0.51	0.63	0.0	0.001	0.476	51.11	107.46	638.82

VALUES AVERAGED OVER ONE PERIOD DM= 5.0

```

SUBROUTINE FORM ( COSOMZ , NT )
DIMENSION COSOMZ(637)
DO 2 COSOMZ(J) = SIN( 6.2832 * J / FLOAT( NT ) + PHASE)
RETURN
END
    
```

FIG. 7B

ISN	0002	0.1253	0.1074	0.2407	0.3090	0.3681	0.4258	0.4818	0.5358	0.5879
COSOMZ	0.0628	0.6845	0.7290	0.7705	0.8090	0.8443	0.8763	0.9048	0.9298	0.9511
	0.6374	0.5823	0.9921	0.9980	1.0000	0.9980	0.9921	0.9823	0.9686	0.9511
	0.5686	0.9048	0.8763	0.8443	0.8090	0.7705	0.7290	0.6845	0.6374	0.5879
	0.5358	0.4817	0.4258	0.3681	0.3090	0.2407	0.1874	0.1253	0.0628	-0.0000
	-0.0628	-0.1253	-0.1874	-0.2407	-0.3090	-0.3681	-0.4258	-0.4818	-0.5358	-0.5879
	-0.6374	-0.6846	-0.7290	-0.7705	-0.8090	-0.8443	-0.8763	-0.9048	-0.9298	-0.9511
	-0.5686	-0.9823	-0.9921	-0.9980	-1.0000	-0.9980	-0.9921	-0.9823	-0.9686	-0.9511
	-0.9298	-0.9048	-0.8763	-0.8443	-0.8090	-0.7705	-0.7290	-0.6845	-0.6374	-0.5878
	-0.5358	-0.4817	-0.4258	-0.3681	-0.3090	-0.2407	-0.1874	-0.1253	-0.0628	0.0000

7. GOEL program

This program calculates the field and current density profiles for the relaxed state with sinusoidal AC modulation. This program was used to calculate Figs. 2, 3 and 4, in which AC and DC components are compared. In the GOEL program it is assumed that the current density and field components consist of a time independent "DC component" and an "AC component" with sinusoidal time dependence (see eqs. (2.16) and (7.1)). The parabolic partial differential equation (2.12) then yields a system of two coupled ordinary differential equations (7.2) with boundary conditions for $r = 0$ (eq. (7.3)) and $r = a$ (eq. (7.4)). The variables have the same meaning as in the GOEPAR program. Instead of the plasma conductivity profile number P the plasma direct current IGA is read in and the profile number P is then calculated from it. We now describe the method of numerical solution employed in the GOELER and SUCCES subroutines.

Insertion of the equation analogous to eq. (2.16)

$$E_z(r,t) = E_0 + E_c(r) \cos \omega t + E_s(r) \sin \omega t \quad (7.1)$$

in the parabolic partial differential equation (2.12) yields the system

$$\frac{1}{r} \frac{d}{dr} \left[r \frac{d}{dr} E_c \right] = b E_s \quad (7.2a)$$

$$\frac{1}{r} \frac{d}{dr} \left[r \frac{d}{dr} E_s \right] = -b E_c \quad (7.2b)$$

with boundary conditions

$$\left. \frac{d}{dr} E_C \right|_{r=0} = 0 \quad (7.3a)$$

$$\left. \frac{d}{dr} E_S \right|_{r=0} = 0 \quad (7.3b)$$

$$E_C|_{r=a} = E_a = V_{PL}/2\pi R \quad (7.4a)$$

where $E_S|_{r=a} = 0, \quad (7.4b)$

$$b = \mu_0 \sigma \omega \quad (7.5)$$

Here b depends via σ on r .

The equations are solved numerically, by reducing the boundary value problem ((7.2) to (7.4)) to an initial value problem in which boundary condition (7.4) is replaced by

$$E_C|_{r=0} = C_0 \quad , \quad (7.6a)$$

$$E_S|_{r=0} = S_0 \quad . \quad (7.6b)$$

The designation "initial value problem" for eq. (7.2, 7.3 and 7.6) comes from the analogy with the initial value problem of mechanics, where the location and velocity of a mass point at time $t = 0$ are given.

We thus have to look for the "initial values" C_0 and S_0 .

Because the differential equation (7.2) to be solved is linear and homogeneous, the boundary values on the right are linear and homogeneous functions of C_0 and S_0 :

$$E_C|_{r=a} = A_{11} C_0 + A_{12} S_0 \quad (7.7a)$$

$$E_S|_{r=a} = A_{21} C_0 + A_{22} S_0 \quad (7.7b).$$

$$\text{For } C_0 = 1 \text{ one has } E_C|_{r=a} = A_{11} \quad (7.8a)$$

$$S_0 = 0 \quad E_S|_{r=a} = A_{21} \quad (7.8b)$$

$$\text{for } C_0 = 0 \text{ one has } E_C|_{r=a} = A_{12} \quad (7.9a)$$

$$S_0 = 1 \quad E_S|_{r=a} = A_{22} \quad (7.9b)$$

The SUCCES subroutine solves the initial value problem. First we use SUCCES to calculate A_{11} and A_{21} according to eq. (7.8), then to calculate A_{12} and A_{22} according to eq. (7.9). We then put the boundary conditions (7.4) in the left-hand side of eq. (7.7) and solve eq. (7.7) for C_0 and S_0 . The third call of SUCCES then yields E_c and $E_s(r)$.

8. SUCCES subroutine

The SUCCES subroutine solves the initial value problem, i.e. eqs. (7.2, 7.3 and 7.6) from Sec. 7. The arguments have the following meanings:

$$C_A = E_C|_{r=0} = \text{initial value for } E_C$$

$$S_A = E_S|_{r=0} = \text{initial value for } E_S$$

$$EC_L = E_C|_{r=a} = \text{right-hand boundary value of } E_C$$

$$ES_L = E_S|_{r=a} = \text{right-hand boundary value of } E_S.$$

EC_L and ES_L are to be calculated by SUCCES routine.

The r mesh points are located so that $R(1) = 0$.

For small r we use the ansatz

$$E_C = C_A + \hat{C}_2 r^2 + \hat{C}_4 r^4 \quad (8.1a)$$

$$E_S = S_A + \hat{S}_2 r^2 + \hat{S}_4 r^4 \quad (8.1b)$$

and determine the coefficients \hat{C}_2 , \hat{C}_4 , \hat{S}_2 and \hat{S}_4 from the differential equation (7.2).

For $r \geq R(3)$ we use a difference scheme:

Let $C(K) = E_C(R_K)$;

one then has

$$\begin{aligned} \frac{1}{r} \frac{d}{dr} \left[r \frac{d}{dr} E_C \right]_{r=R(K)} &= \frac{r_{K+1/2} \frac{C_{K+1} - C_K}{r_{K+1} - r_K} - r_{K-1/2} \frac{C_K - C_{K-1}}{r_K - r_{K-1}}}{r_K (r_{K+1/2} - r_{K-1/2})} \\ &= b E_S(R(K)) = b S_K, \end{aligned} \quad (8.2)$$

where $S_k = E_S(r=R(K))$,

$$r_K = R(K)$$

and $r_{K+1/2} = \frac{1}{2}(R(K) + R(K+1))$.

We solve the difference equation (8.2) for C_{K+1} , and also the analogous difference equation describing E_S for S_{K+1} . The values of E_C and E_S are known for K and $K-1$, either from the previous step or from eq. (8.1) for small r .

List of input parameters

We now review the parameters used for calculating the curves in Figs. 2 to 8. This is necessary if these curves are to be reproduced with the programs presented in this report. The respective figure captions

are not sufficient. It is very difficult, for example, with the current modulation ΔI given in Fig. 3 to arrive at the AC voltage V_C used as a parameter in producing Fig. 3.

1) Constant parameters

Limiter radius	AL = 0.11 metre
Toroidal field	BTOR = 2.8 tesla
Plasma direct current	IGA = 55.kA
Major radius	RG = 0.7 metre
Conductivity (r=0)	SIG0 = $1.44 \cdot 10^7 \text{ ohm}^{-1} \text{ m}^{-1}$
DC voltage	VG = 2.2 Volt

2) Parameters which vary from curve to curve

FIG	A	FR	ωt	VC	program
2	0.13	100		29.	GOEL
				60.	
				131.	
3	0.13	400	0.	18.	GOEL
			1.57		
			3.14		
			4.71		
4	0.11	300		50.	GOEL
			0.13		
			0.25		
5	0.13	400		4.5	GOEL GOEPAR
				9.	
				18.	
6	0.13	400		9.	GOEPAR
		4000		36.	
7	0.13	400		3.	GOEPAR
				4.5	
				9.	
8	0.13	400.		2.8	GOEPAR

Remarks:

In program GOEPAR we have used P as an input parameter instead of $IGA = I_{PLO}$ (see eq. (2.8)). From $IGA = 55$ and $A = .13$ it follows that $P = 5.76$.

```

C WECHSELSTRCMPROFILE, ALTERNATING CURRENT , SEGMENT   G C E L
ISN 0002 REAL*4      IGA, JO, J1, JG, JZ, LAMBDA ,MO, N1, NG
ISN 0003 COMMON /GOE/  R(51) , BA , P , V , LMAX
ISN 0004 COMMON /SUC/  B(51) , EC(51) , ES(51)
ISN 0005 10 PRINT 58
ISN 0006 PRINT 92
ISN 0007 READ 112,  A, AL, BTCR, DR, FR, IGA, OMT, RG, SIGO, VC, VG
ISN 0008 PRINT 113,  A, AL, BTCR, DR, FR, IGA, CMT, RG, SIGO, VC, VG
ISN 0009 LMAX = 1.2 + 1./DR
ISN 0010 LI = LMAX - 1
ISN 0011 MO = 1.25664E-6
ISN 0012 IGA = IGA * 1.E3
ISN 0013 SIGO = SIGO* 1.E7
ISN 0014 OM = 6.2832 * FR
ISN 0015 COSOMT = CCS( CMT)
ISN 0016 SINOMT = SIN( CMT)
ISN 0017 BA = MO * SIGO * OM * AL**2
ISN 0018 LAMBDA = SQRT ( 1. / BA )
ISN 0019 V = (AL/A)**2
ISN 0020 EO = VC / (6.2832 *RG)
ISN 0021 EG = VG / (6.2832 *RG)
ISN 0022 P = 3.1416 * SIGO * EG * AL**2 / (V* IGA) - 1.
ISN 0023 DO 1 L=1,LMAX
ISN 0024 R(L) = DR* (L-1)
ISN 0025 RQ = R(L)**2
ISN 0026 1 B(L) = BA* (1.- V*RQ)**P
ISN 0027 CALL SUCCES ( 1. , 0. , A11 , A21 )
ISN 0028 CALL SUCCES ( 0. , 1. , A12 , A22 )
ISN 0029 DET = A11 *A22 - A21 *A12
ISN 0030 CO = EO * A22 / DET
ISN 0031 SO = - EO * A21 / DET
ISN 0032 CALL SUCCES ( CC , SO , A3 , A4 )
ISN 0033 PRINT 91
ISN 0034 PRINT 113,  LAMBDA , P , V
ISN 0035 PRINT 93
ISN 0036 JO = SIGO *EG
ISN 0037 DO 3 L=1,L1
ISN 0038 RQ = R(L)**2
ISN 0039 SIG = SIGO* (1.- V*RQ)**P
ISN 0040 J1 = SIG* SQRT( ES(L)**2 + EC(L)**2 )
ISN 0041 JG = SIG* EG
ISN 0042 JZ = SIG*(EG + ES(L) *SINCMT + EC(L) *COSOMT)
ISN 0043 NG = JG / JO
ISN 0044 N1 = J1 / JO
ISN 0045 3 PRINT 110,  R(L) , SIG , J1, N1, JG, NG, JZ
ISN 0046 GO TO 10
ISN 0047 91 FORMAT(/31H LAMBDA P V)
ISN 0048 92 FORMAT(/110H A AL BT CR DR FR
1 IGA OMT RG SIGO VC VG)
ISN 0049 93 FORMAT(/71H R SIG J1 N1 JG
1 NG JZ)
ISN 0050 98 FORMAT( 1H1)
ISN 0051 110 FORMAT ( F12.3 , 1P2E10.2 , 0PF8.3 , 1PE12.2 , 0PF8.3 , 1PE12.2)
ISN 0052 112 FORMAT ( 12F6.3)
ISN 0053 113 FORMAT ( F12.3, 11F10.3)
ISN 0054 END

```

```

ISN 0002 SUBROUTINE SUCCES ( CA, SA, ECL, ESL)
ISN 0003 COMMON /GOE/  R(51) , BA , P , V , LMAX
ISN 0004 COMMON /SUC/  B(51) , EC(51) , ES(51)
ISN 0005 EC(1) = CA
ISN 0006 ES(1) = SA
ISN 0007 LM = LMAX - 1
ISN 0008 C2 = 0.25 * BA* SA
ISN 0009 S2 = - 0.25 * BA* CA
ISN 0010 C4 = 0.0625 * BA*(S2 -P*SA)
ISN 0011 S4 = - 0.0625 * BA*(C2 -P*CA)
ISN 0012 R2 = R(2)**2
ISN 0013 EC(2) = CA + R2*( C2 + C4*R2)
ISN 0014 ES(2) = SA + R2*( S2 + S4*R2)
ISN 0015 DO 3 K=2,LM
ISN 0016 QP = ( R(K+1) + R(K)) / ( R(K+1) - R(K))
ISN 0017 QM = ( R(K-1) + R(K)) / ( R(K-1) - R(K))
ISN 0018 QMQP = QM / QP
ISN 0019 T = R(K) * ( R(K+1) - R(K-1)) * B(K) / QP
ISN 0020 ECL =EC(K) + (EC(K-1) -EC(K)) * QMQP + T*ES(K)
ISN 0021 ESL =ES(K) + (ES(K-1) -ES(K)) * QMQP - T*EC(K)
ISN 0022 EC(K+1) = ECL
ISN 0023 ES(K+1) = ESL
ISN 0024 3 CONTINUE
ISN 0025 RETURN
ISN 0026 END

```


A	AL	BTOR	DR	FR	IGA	OMT	RG	SIGO	VC	VG
0.130	0.110	2.800	0.025	1000.000	55.000	0.0	0.700	1.400	131.300	2.200
LAMBDA	P	V								
0.027	5.760	0.716								
R	SIG	J1	N1	JG	NG	JZ				
0.0	1.40E+07	9.23E+02	0.000	7.00E+06	1.000	7.00E+06				
0.025	1.40E+07	9.31E+02	0.000	6.98E+06	0.997	6.99E+06				
0.050	1.39E+07	1.10E+03	0.000	6.53E+06	0.990	6.53E+06				
0.075	1.37E+07	1.62E+03	0.000	6.84E+06	0.977	6.84E+06				
0.100	1.34E+07	2.65E+03	0.000	6.72E+06	0.959	6.72E+06				
0.125	1.31E+07	4.45E+03	0.001	6.56E+06	0.937	6.56E+06				
0.150	1.27E+07	7.51E+03	0.001	6.38E+06	0.911	6.37E+06				
0.175	1.23E+07	1.27E+04	0.002	6.16E+06	0.880	6.15E+06				
0.200	1.18E+07	2.13E+04	0.003	5.92E+06	0.846	5.90E+06				
0.225	1.13E+07	3.54E+04	0.005	5.66E+06	0.808	5.64E+06				
0.250	1.08E+07	5.81E+04	0.008	5.38E+06	0.768	5.37E+06				
0.275	1.02E+07	9.39E+04	0.013	5.08E+06	0.726	5.11E+06				
0.300	9.54E+06	1.49E+05	0.021	4.77E+06	0.681	4.88E+06				
0.325	8.90E+06	2.32E+05	0.033	4.45E+06	0.636	4.68E+06				
0.350	8.25E+06	3.54E+05	0.051	4.13E+06	0.589	4.47E+06				
0.375	7.60E+06	5.26E+05	0.075	3.80E+06	0.543	4.17E+06				
0.400	6.95E+06	7.64E+05	0.109	3.47E+06	0.496	3.72E+06				
0.425	6.31E+06	1.08E+06	0.154	3.15E+06	0.450	3.03E+06				
0.450	5.68E+06	1.49E+06	0.213	2.84E+06	0.406	2.69E+06				
0.475	5.07E+06	1.99E+06	0.285	2.54E+06	0.362	2.40E+05				
0.500	4.50E+06	2.59E+06	0.371	2.25E+06	0.321	-2.56E+05				
0.525	3.95E+06	3.28E+06	0.468	1.97E+06	0.282	-1.29E+06				
0.550	3.43E+06	4.02E+06	0.574	1.72E+06	0.245	-1.94E+06				
0.575	2.95E+06	4.78E+06	0.682	1.48E+06	0.211	-2.67E+06				
0.600	2.51E+06	5.50E+06	0.786	1.26E+06	0.180	-1.61E+06				
0.625	2.12E+06	6.14E+06	0.876	1.06E+06	0.151	-6.48E+05				
0.650	1.76E+06	6.63E+06	0.947	8.79E+05	0.126	6.29E+05				
0.675	1.44E+06	6.53E+06	0.990	7.20E+05	0.103	2.00E+06				
0.700	1.16E+06	7.00E+06	1.000	5.81E+05	0.083	3.23E+06				
0.725	9.23E+05	6.84E+06	0.977	4.62E+05	0.066	4.15E+06				
0.750	7.19E+05	6.45E+06	0.921	3.60E+05	0.051	4.67E+06				
0.775	5.49E+05	5.87E+06	0.838	2.75E+05	0.035	4.79E+06				
0.800	4.10E+05	5.14E+06	0.734	2.05E+05	0.029	4.55E+06				
0.825	2.98E+05	4.33E+06	0.618	1.49E+05	0.021	4.64E+06				
0.850	2.11E+05	3.50E+06	0.499	1.06E+05	0.015	3.38E+06				
0.875	1.44E+05	2.70E+06	0.385	7.21E+04	0.010	2.67E+06				
0.900	9.47E+04	1.98E+06	0.283	4.74E+04	0.007	1.59E+06				
0.925	5.94E+04	1.37E+06	0.196	2.97E+04	0.004	1.39E+06				
0.950	3.53E+04	8.95E+05	0.128	1.76E+04	0.003	9.09E+05				
0.975	1.95E+04	5.40E+05	0.077	9.77E+03	0.001	5.45E+05				

FIG. 2

References

- /1/ H.P. FURTH, J.KILLEEN, and M.N.ROSENBLUTH,
Phys. Fluids 6, 459-484 (1963)
- /2/ H.P.FURTH, P.H.RUTHERFORD, and H.SELBERG,
Phys. Fluids 16, 1054-1063 (1973)
- /3/ R.B.WHITE, D.A.MONTICELLO, M.N.ROSENBLUTH, and B.V.WADDELL,
Phys. Fluids 20, 800-805 (1977)
- /4/ G.BATEMAN, MHD Instabilities, MIT Press (1978)
- /5/ A.H.GLASSER, J.M.GREENE, J.L.JOHNSON, Phys.Fluids 19, 567-574 (1976)
- /6/ J.M.FINN, Nuclear Fusion 15, 845-854 (1975)
- /7/ A.B.RECHESTER, T.H.STIX, Phys.Rev.Lett. 36, 587-591 (1976)
- /8/ B.V.WADDELL, B.CARRERAS, H.R.HICKS and HOLMES,
Phys. Fluids 22, 5, (1979)
- /9/ R.JAENICKE, H.WOBIG, to be published
Proc. 9. European Conf. Oxford (1979)
- /10/ J.D.CALLEN, Proc. 7.Int.Conf. Innsbruck (1978)
Vol. 1, IAEA Vienna (1979), p. 415
- /11/ R.D.RICHTMYER and K.W.MORTON, Difference Methods for Initial
Value Problems, Interscience Publishers, John Wiley & Sons,
New York 1957
- /12/ R.BECKER, Theorie der Elektrizität, 1. Band, § 58
Teubner'sche Verlagsgesellschaft, Stuttgart, 1957
- /13/ P.H.RUTHERFORD, Phys.Fluids 16, 1903 (1973)
- /14/ S. v.GOELER et al., Proceedings of Symposium on Disruptive
Instabilities, Garching (1979)
- /15/ S. v.GOELER et al., Proceedings of 9. European Conference on
Controlled Fusion and Plasma Physics, Oxford, 17-21.9.1979.